



Phase transition pathways of the hydrates of magnesium sulfate in the temperature range 50°C to 5°C: Implication for sulfates on Mars

Alian Wang,¹ John J. Freeman,¹ and Bradley L. Jolliff¹

Received 19 September 2008; revised 5 December 2008; accepted 5 January 2009; published 25 April 2009.

[1] Dehydration/rehydration experiments were conducted on pure Mg-sulfates and mixtures of epsomite with Ca-sulfates, Fe-sulfates, Fe-oxide, and Fe-hydroxide. The goal was to investigate the stabilities and phase transition pathways of Mg-sulfate hydrates, under temperature and relative humidity conditions relevant to Mars, as a function of starting structure and coexisting species. Two pathways were found to form Mg-sulfate monohydrates between 5°C and 50°C through dehydration of epsomite or hexahydrite. Two polymorphs of Mg-sulfate monohydrates were characterized in this study. It is important to distinguish among these phases on Mars because they have different formation conditions that have the potential to provide additional information on surface and subsurface geologic processes. We found that Mg-sulfates with moderate hydration states (especially starkeyite and amorphous Mg-sulfates) can be very stable under current Martian surface conditions. On the basis of NIR spectral features, these phases are good candidates for polyhydrated sulfates identified on Mars by OMEGA and CRISM; thus, they may contribute to the high hydrogen concentrations found by the neutron spectrometer on the orbiting Odyssey spacecraft. Our experiments indicate that the maximum number of water molecules per SO₄ held by the amorphous Mg-sulfate structure is three. In addition, the amorphization rate of Mg-sulfates is strongly dependent on temperature. The low temperature (approximately −80°C) in the early morning hours during the Martian diurnal cycle would slow the dehydration rate, which would favor the stability of starkeyite over amorphous Mg-sulfates and would lead to a low abundance of the latter.

Citation: Wang, A., J. J. Freeman, and B. L. Jolliff (2009), Phase transition pathways of the hydrates of magnesium sulfate in the temperature range 50°C to 5°C: Implication for sulfates on Mars, *J. Geophys. Res.*, 114, E04010, doi:10.1029/2008JE003266.

1. Introduction

[2] Sulfate minerals are important records of past and current environmental conditions on the Martian surface and in its subsurface. They play a critical role in the sulfur cycle, surface processes, and hydrologic history of Mars. Many reports from recent missions have documented the occurrence of sulfates on Mars. Kieserite (MgSO₄·H₂O), gypsum (CaSO₄·2H₂O), and bassanite (2CaSO₄·H₂O) were identified by the OMEGA instrument on Mars Express [Arvidson *et al.*, 2005; Bibring *et al.*, 2005; Gendrin *et al.*, 2005; Langevin *et al.*, 2005] and by the CRISM instrument on the Mars Reconnaissance Orbiter [Murchie *et al.*, 2007a; Lichtenberg *et al.*, 2008; Roach *et al.*, 2007, 2008; Wiseman *et al.*, 2007]. The label “polyhydrated sulfates” was assigned to a less specific spectral pattern, and they can be attributed to various hydrated Mg-sulfates and multication sulfates [Gendrin *et al.*, 2005]. On a global scale, sulfates have mainly been found in the region of Valles

Marineris and at Meridiani Planum [Bibring *et al.*, 2006a, 2006b]. Of interest is an apparent systematic trend in the occurrence of different types of sulfates at regional scales. Each type of sulfate seems to have a distinct geomorphic setting with sharp contacts [Mangold *et al.*, 2006, 2007]. Kieserite has been found mostly on steep slopes or on plateaus, whereas polyhydrated sulfate occur on shallow slopes or on valley floors. A large patch of gypsum was found in a region near the North Pole [Langevin *et al.*, 2005] and on the top of hills in Valles Marineris. This trend indicates a potential commonality in the geological processes that were responsible for the deposition and phase transitions among these sulfates during Martian history.

[3] At the Meridiani Planum Opportunity rover exploration site, sulfates are a major constituent of Meridiani outcrops [Squyres *et al.*, 2006a]. Mineral modeling based on Alpha Particle X-Ray Spectrometer (APXS) and Mössbauer spectrometer data indicate that Meridiani outcrop rocks contain some 35–36 wt % sulfates, consisting of Mg-sulfates, Fe-sulfates (jarosite), and Ca-sulfates, in order of decreasing abundance [Clark *et al.*, 2005]. The compositional and mineralogical features are relatively consistent in the Meridiani outcrop rocks encountered by Opportunity throughout its 13.6 km traverse (until sol 1715). Combined

¹Department of Earth and Planetary Sciences and the McDonnell Center for the Space Sciences, Washington University, St. Louis, Missouri, USA.

observations [Arvidson *et al.*, 2006a] of orbital imaging (OMEGA and CRISM) and surface exploration (MER) suggests that the same type of outcrop could extend several hundred kilometers across Meridiani Planum and hundreds of meters in depth.

[4] At Gusev Crater, sulfates have been found in rocks at specific locations [Squyres *et al.*, 2006b; Wang *et al.*, 2006a] and in the salty soils excavated by Spirit at more than 10 locations [Arvidson *et al.*, 2006b, 2008; Haskin *et al.*, 2005; Wang *et al.*, 2006b, 2008]. Large variations in composition and mineralogy occur in the Gusev sulfates. Mössbauer spectral analysis suggests the existence of a ferric sulfate in some of the salty soils [Morris *et al.*, 2006a, 2008]. Mineral modeling [Ming *et al.*, 2006, 2008; Wang *et al.*, 2006a; 2006b; Yen *et al.*, 2008], based on APXS and Mössbauer data, also indicates the existence of Mg- and Ca-sulfates in these Gusev targets. Moreover, major cations in the sulfates of different targets at different locations correlate with the degree of alteration of local rocks [Wang *et al.*, 2008a]. Miniaturized Thermal Emission Spectrometer observations indicate that the sulfates are hydrated. However, no further information on the hydration states of these sulfates and on their mineralogy can be extracted from the data obtained by the instruments onboard the Spirit rover.

[5] As stated by McLennan *et al.* [2007], the discovery of the widespread occurrence of sulfates on Mars and almost no carbonates (at least at the surface) suggests that the sulfur cycle, rather than a carbon cycle, dominates surficial processes on Mars. Compared to weak carbon-based acids (i.e., carbonic acid, organic acids), sulfuric acid is very strong. A small amount of sulfuric acid would result in highly acidic aqueous solutions that can readily alter Martian surface materials. The fact that most of the sulfate deposits on Mars are ancient suggests that they may have been a major sink of acidity for much of Mars' history. Therefore, the S cycle could have played a critical role in many surface processes (up to the present), involving both igneous rocks (mainly basalts) [McSween *et al.*, 2004, 2006] and sedimentary materials, e.g., the phyllosilicates recently reported by the CRISM team [Bishop *et al.*, 2008; Ehlmann *et al.*, 2008; Mustard *et al.*, 2008].

[6] Although these mission observations have demonstrated the importance of sulfate mineralogy to Mars science, there are discrepancies between the findings of orbital remote sensing and surface exploration. Questions remain regarding the lack of detection of Fe-sulfates from orbit and the non-detection of sulfates at the Opportunity site (Meridiani) by orbiters, contrary to the findings by the rovers on the surface. Another unknown is the source of high levels of hydrogen detected by the neutron spectrometer (NS) on the Mars Odyssey orbiter, specifically in the two equatorial regions of exploration by Spirit and Opportunity. Although it is likely that the sulfate minerals contain waters of hydration, they have not been detected directly.

[7] On the basis of mission data, knowledge of the S cycle during surface processes on Mars remains limited. Processes and conditions associated with formation, phase transitions, and survival of various Martian sulfates, as well as the role of Martian sulfates in hosting water in Martian equatorial or other regions, are not well known. This gap in knowledge can be addressed through laboratory simulation experiments. These experiments provide information on the stability fields

and phase boundaries of various hydrated sulfates and on the phase transition pathways under conditions relevant to Martian surface and subsurface environments [Chipera and Vaniman, 2007; Chou and Seal, 2003, 2007; Freeman *et al.*, 2007, 2008; Ling *et al.*, 2008a, 2008b; Tosca *et al.*, 2004, 2008; Tosca and McLennan, 2006; Wang *et al.*, 2006c, 2007, 2008; Vaniman *et al.*, 2004; Vaniman and Chipera, 2006]. Experiments and geochemical models [Tosca *et al.*, 2005] also provide hypotheses and evidence on evaporites and their mineral deposition sequences from acidic fluids derived from the weathering of igneous rocks with compositions of those thought to occur on Mars.

[8] In a previous paper [Wang *et al.*, 2006c], we developed methods to control and monitor the variation of hydration states of Mg-sulfates in laboratory simulation experiments for the purpose of studying the stability fields and phase transition pathways of a full range of hydrated Mg-sulfates that could be anticipated to occur on Mars. Our unique approach is by using multiple spectroscopic techniques to connect laboratory simulations with surface exploration results and orbital remote sensing data. The spectroscopic techniques that we used included Raman spectroscopy, X-ray diffraction (XRD), mid-IR attenuated total reflectance (ATR), and NIR diffuse reflectance spectroscopy. During the primary phase of this study [Wang *et al.*, 2006c], the characteristic Raman spectral patterns were obtained from eleven distinct Mg-sulfates, hydrated and anhydrous, crystalline and amorphous, whose identities were confirmed by XRD. The unique Raman spectral feature of each Mg-sulfate allows its direct identification, either alone or in mixtures such as those occurring during the intermediate stages of a dehydration/rehydration process. Therefore, noninvasive Raman measurements can be used to study phase transition pathways of hydrated Mg-sulfates as reported here. We compare the information from mid-IR ATR with Raman spectra of the same sample to study the fundamental vibrational modes for the purpose of phase identification and characterization. We used NIR (1–5 μm) reflectance measurements on these well characterized samples to obtain spectral features in the region of overtone and combinational modes. These reflectance measurements are compared with the NIR reflectance spectra from orbital remote sensing (OMEGA and CRISM) on Mars.

[9] In this study, we use the same methods to investigate the stability field and phase transition pathways of four hydrates of Mg-sulfate and mixtures of Mg-sulfate with Ca- and Fe-sulfates and Fe-oxides and Fe-hydroxides. Analytical grade chemicals were used directly or to synthesize the starting hydrated Mg-sulfate phases, as well as the Ca- and Fe-sulfates used in mixing experiments. Humidity buffer techniques were used to maintain stable relative humidity (RH) levels at fixed temperatures. Noninvasive microbeam Raman spectroscopy and gravimetric measurements were used for monitoring the dehydration/rehydration processes and for making phase identifications at the intermediate and final stages of equilibrium. XRD and mid-IR ATR measurements provide clarification on the structures suggested by their Raman spectra. Near-IR reflectance spectra were obtained from certain samples in order to compare with OMEGA and CRISM spectra. The details of the samples, the dehydration/rehydration experiments, and phase identifications are described in the Appendix.

Table 1. Relative Humidity in Humidity Buffers at Three Temperatures^a

| | 50°C | 21°C | 5°C |
|-----------------------------------|------|------|------|
| LiBr | 5.5 | 6.6 | 7.4 |
| LiCl | 11.1 | 11.3 | 11.3 |
| LiI | 12.4 | 18.4 | 21.7 |
| MgCl ₂ | 30.5 | 33.0 | 33.6 |
| NaI | 29.2 | 39.4 | 42.4 |
| Mg(NO ₃) ₂ | 45.4 | 54.1 | 58.9 |
| NaBr | 50.9 | 58.8 | 63.5 |
| KI | 64.5 | 69.7 | 73.3 |
| NaCl | 74.4 | 75.4 | 75.7 |
| KCl | 81.2 | 85.0 | 87.7 |
| KNO ₃ | 84.8 | 94.4 | 96.3 |
| H ₂ O | 100 | 100 | 100 |

^aValues are in % RH.

[10] The emphasis of the current study is (1) to understand the formation pathway(s) of Martian Mg-sulfate monohydrate in a middle- to low-temperature range, (2) to determine the potential stability of Mg-sulfates with intermediate hydration degrees in RH-T ranges relevant to Martian surface/subsurface conditions, and (3) to determine the role of amorphous hydrated Mg-sulfates in the related phase transition processes.

2. Design of Hydration/Dehydration Experiments and General Results

[11] In this section, we describe the general results of 120 hydration/dehydration experiments begun from four hydrates of Mg-sulfate, which were done at three temperatures (5°C, 21°C, and 50°C) with 10 controlled RH levels at each temperature (Table 1). In addition, the results from 18 experiments using mixtures of epsomite with Ca-sulfate and ferric sulfates, Fe-hydroxide, and Fe-oxide as starting phases and done at 50°C and two RH levels (11% and 31%) will also be discussed. Among these 138 experiments, 12 experiments at 5°C started with four Mg-sulfate hydrates and three controlled RH levels are continuing at the time of writing.

[12] Four factors were considered when designing these experiments. The first factor is partial water pressure. Our experiments were done under Earth atmospheric pressure, with well-controlled RH. Compared with atmospheric pressure and partial water pressure on Mars, our experimental conditions would increase the reaction rates of the hydration/dehydration processes, but would not change the results on stability fields of different hydrates of Mg-sulfate and their phase transition pathways. Although the enthalpy of a reaction is a function of pressure, the small pressure difference between Mars and Earth has only a negligible effect. Moreover, running the experiments at higher pressure would help to complete hydration/dehydration processes with a reasonable duration in the laboratory.

[13] The second factor is temperature. The stability fields of different hydrates of Mg-sulfate and their phase transition pathways would be affected by temperature. Our experiments were done over a temperature range from 5°C to 50°C. The selection of this temperature range was based on a compromise between higher reaction rates (to reach equilibrium in a reasonable time) and maintaining a level of similarity to Mars' surface temperature range. The maximum daytime

ground temperature at Gusev Crater and Meridiani Planum measured by Spirit and Opportunity is about 295 K (22°C), with Meridiani slightly warmer than Gusev [Smith *et al.*, 2006]. The minimum nighttime ground temperature is around 185 K (−88°C) [Smith *et al.*, 2004]. The temperature range (5–50°C) of our experiments covers the higher portion of the surface temperature range on Mars. We are gradually working toward a lower temperature range. A set of 30 experiments at −10°C (with five starting Mg-sulfates in six controlled RH buffers) has been running in our lab for over 5000 h. These reactions are very slow and ongoing, and the results will be reported later. In addition, conducting experiments at three different temperatures (including 50°C) allows us to observe the tendency of phase transitions as a function of temperature, especially for the metastable phase(s) in the middle to low RH range. This will help us understand the general mechanism of these phase transitions, and allow us to predict (when possible) the phase transitions at lower temperatures.

[14] The third factor is the starting phase. In the middle to low temperature range, the structures of starting phases affect the development of the phase transitions, which affect the hydration state of Mg-sulfates at the intermediate and end stages of equilibria. The starting Mg-sulfate phases in our experiments were chosen on the following basis: (1) the phase has been identified on Mars, e.g., monohydrate Mg-sulfate (1w); (2) the phase is a normal precipitation product from aqueous solution at middle to low temperature range, e.g., epsomite (7w); (3) the phase has been observed in terrestrial natural occurrences, e.g., starkeyite (4w); and (4) the phase has been proposed to occur during rapid and wide RH swings in the diurnal cycle on Mars, e.g., amorphous Mg-sulfates (Am). Meridianiite MgSO₄·11H₂O was suggested [Peterson and Wang, 2006] to be present in Martian polar regions, and this was used as one of the starting phases for our experiments at −10°C; the results of experiments involving meridianiite will be reported in a subsequent paper.

[15] In a simulation experiment, a limited numbers of factors would normally be included in order to understand the major controlling mechanism. T, RH, and the structures of starting phases were the three major factors in our experimental design. However, in the real world, the phase transition of a hydrated Mg-sulfate can be affected by many other factors. One of the potentially important factors is the coexisting hydrated and anhydrous mineral phases, which may function as a local RH buffer (perhaps at a microscopic scale) surrounding a grain of Mg-sulfate. On Mars, the coexistence of Mg-, Fe-, and Ca-sulfates is indicated by orbital observations [Gendrin *et al.*, 2005] and has been inferred from mineral modeling calculations based on compositional information (APXS and Mössbauer) [Clark *et al.*, 2005; Ming *et al.*, 2006; Wang *et al.*, 2006a, 2006b; Yen *et al.*, 2008]. To evaluate the potential effect of coexisting phases, mixtures of powders of epsomite with three Ca-sulfates, as well as with ferrous and ferric sulfates, hematite, and goethite, were used as starting phases for dehydration experiments at fixed RH and T conditions.

2.1. Dehydration of Epsomite (MgSO₄·7H₂O)

[16] Dehydration experiments of epsomite (7w, MgSO₄·7H₂O) at 50°C, 21°C, and 5°C were run for 1979, 1979, and 18629

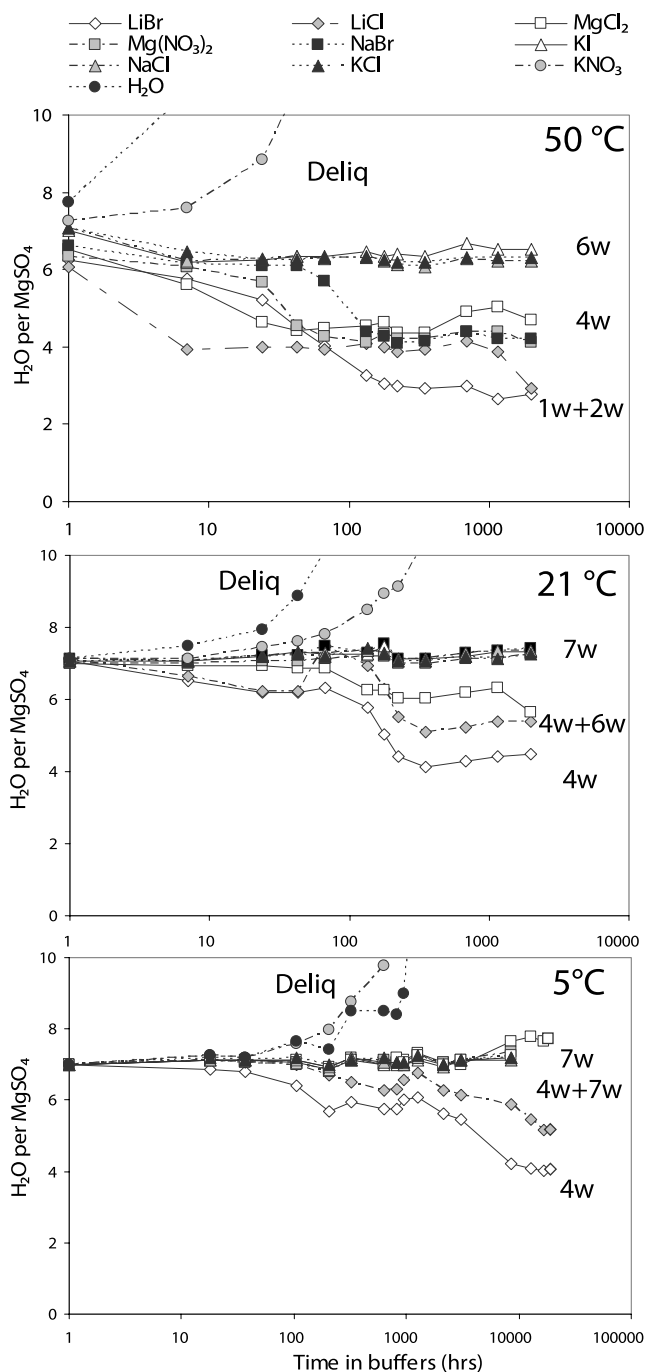


Figure 1. Gravimetric measurement results (water molecule per MgSO_4) during dehydration of epsomite at 50°C , 21°C , and 5°C .

h respectively. Figure 1 shows the results of gravimetric measurements, expressed in water molecules per MgSO_4 versus the hours of reaction when the samples were kept in RH buffers. These graphs suggest that after ~ 1000 h, most of the experiments had reached equilibrium. Exceptions include one experiment in the LiCl buffer at 50°C and one in the MgCl_2 buffer at 21°C . Because of the slow reaction rate at low temperature (5°C), it is uncertain that equilibrium in the LiBr, LiCl, and MgCl_2 buffers at 5°C is actually reached. Therefore, these three experiments are continuing

at the time of writing, as well as those begun with the other three Mg-sulfate hydrates (1w, 4w, and Am). Table 2 lists the phase transition pathway during the dehydration of epsomite. Every phase in this table was identified by Raman spectroscopy, as a function of time during the development of equilibrium.

[17] The last rows in each of the three temperature sections in Table 2 show the final Mg-sulfate phases of the experiments. For the systems equilibrated at high RH ($>50\%$, 19 experiments), the final hydration states (7w, 6w, or deliquescence) were consistent with the stability fields and phase boundaries determined previously by *Chou and Seal* [2003]. The phase transition pathways at high RH were straightforward; that is, the starting materials either remained as 7w or directly converted to 6w, or to deliquescence (deliq).

[18] For the systems equilibrated at low RH ($\leq 50\%$, 11 experiments), Table 2 shows that starkeyite (4w) was the final phase in eight experiments, but the pathway of dehydration can be complicated. At all three temperatures, the 7w to 6w phase transition occurred readily. When dehydration continued, 6w converted to 4w and stayed as 4w in most cases. At 50°C and with extremely low RH ($\leq 10\%$), amorphous Mg-sulfate (Am) started to form (Table 2 and Figure 2). At intermediate stages, further dehydration and recrystallization of Am produced pentahydrate (5w, $\text{MgSO}_4 \cdot 5\text{H}_2\text{O}$), 4w, sanderite (2w, $\text{MgSO}_4 \cdot 2\text{H}_2\text{O}$), and monohydrate (1w). 1w and 2w Mg-sulfates were the final equilibrated phases at 6% RH and 11% RH for 50°C experiments (Figure 2). When coexisting with Am, 6w can persist (>686 h), even under very dry conditions (6% RH and 50°C). On the other hand, in pure form, 6w converted totally to 4w after 24 h in relatively dry conditions (11–31% RH at 50°C , Table 2).

[19] In a previous study, we suggested that the stable substructural unit in starkeyite (4w), the four-member rings made by two (SO_4) and two $\text{Mg}(\text{O}_2(\text{OH})_4)$, must have raised the activation energy for further dehydration [*Wang et al.*, 2006c]. In the middle to low temperature range (5 to 50°C in our experiments), there is not enough energy to break down the four-member ring and to form crystalline Mg-sulfates with lower degree of hydration such as kieserite (1w). This could be the reason that 4w is the major dehydration product from 7w at low RH-T. When Am forms under extremely dry conditions, however, its irregular structural framework would reduce the activation energy needed for further phase transformation. Thus, low-degree hydrates of different crystal structures, such as 1w and 2w, can be formed from Am (Figure 2).

[20] On the basis of reaction pathways (Table 2) and gravimetric variations (Figure 1), we can estimate the possible equilibrium phases for the few experiments that appear not to have reached equilibrium: 1w plus 2w for the system at 50°C in the LiCl buffer, and 4w for the system at 21°C in the MgCl_2 buffer. Among the ten experiments done at 5°C , after 12802 h, 6w was still present in the system in the lowest RH buffer (LiBr), but 4w became the final phase after 18629 h (Table 2). The system in the MgCl_2 buffer (34% RH) at 5°C occurred in the stability field of 1w as shown by *Chou and Seal* [2003, Figure 3], but 7w was found after 698 days of dehydration. Figure 1 suggests that equilibria in these systems were not reached.

Table 2. Phase Transition Pathways of Epsomite Dehydration at 50°C, 21°C, and 5°C in 10 Humidity Buffers Based on Raman Spectra of the Samples^a

| T = 50°C | | | | | | | | | | |
|----------|------------------------|-------------------|-------------------|-----------------------------------|---------|--------|--------|------|------------------|------------------|
| | LiBr | LiCl | MgCl ₂ | Mg(NO ₃) ₂ | NaBr | KI | NaCl | KCl | KNO ₃ | H ₂ O |
| RH | 5.5 | 11.1 | 30.5 | 45.4 | 50.9 | 64.5 | 74.4 | 81.2 | 84.8 | 100.0 |
| Time (h) | | | | | | | | | | |
| 1 | 6w | 6w | 6w | 6w, 7w | 7w, 6w | 7w, 6w | 7w | 7w | 7w | 7w |
| 7 | 6w, Am | 4w, 6w | 6w, 4w | 6w | 6w | 6w | 6w | 6w | 7w, 6w | deliq |
| 24 | 6w, Am | 4w | 4w | 4w, 6w | 6w | 6w | 6w | 6w | 6w | deliq |
| 43 | 6w, Am | 4w | 4w | 4w, 6w | 6w | 6w | 6w, 7w | 6w | 6w | deliq |
| 67 | 6w, Am, 2w, 1w | 4w | 4w | 4w, 6w | 6w, 4wt | 6w | 6w | 6w | 6w | deliq |
| 134 | 6w, Am, 2w + 1w + 4w | 4w | 4w | 4w | 4w | 6w | 6w | 6w | 6w | deliq |
| 179 | 6w, Am, 5w, 4w, 2w, 1w | 4w | 4w | 4w, 6wt | 4w, 6wt | 6w | 6w | 6w | 6w | deliq |
| 224 | 6w, 4w, 2w, 1w, Am | 4w | 4w | 4w | 4w, 6wt | 6w | 6w | 6w | 6w | deliq |
| 351 | 6w, Am | 4w | 4w | 4w, 6wt | 4w, 6wt | 6w | 6w | 6w | 6w | deliq |
| 686 | 6w, 4w, 2w, 1w, Am | 4w, 2w, 1w | 4w | 4w, 6wt | 4w | 6w | 6w | 6w | 6w | deliq |
| 1143 | 1w, 2w | 4w, 2w, 1w | 4w | 4w | 4w | 6w | 6w | 6w | 6w | deliq |
| 1979 | 1w, 2w | 2w, 1w, 4w | 4w | 4w | 4w | 6w | 6w | 6w | 6w | deliq |
| T = 21°C | | | | | | | | | | |
| | LiBr | LiCl | MgCl ₂ | Mg(NO ₃) ₂ | NaBr | KI | NaCl | KCl | KNO ₃ | H ₂ O |
| RH | 6.6 | 11.3 | 33.0 | 54.1 | 58.8 | 69.7 | 75.4 | 85.0 | 94.4 | 100.0 |
| Time (h) | | | | | | | | | | |
| 1 | 7w | 7w, 6w | 7w | 7w | 7w | 7w | 7w | 7w | 7w | 7w |
| 7 | 6w, 7w | 6w, 7w | 7w | 7w | 7w | 7w | 7w | 7w | 7w | 7w |
| 24 | 6w | 6w, 4wt | 7w | 7w | 7w | 7w | 7w | 7w | 7w | 7w |
| 43 | 6w | 6w | 7w | 7w | 7w | 7w | 7w | 7w | 7w | liq |
| 67 | 6w, 4w | 6w, 4w | 6w, 7w | 7w | 7w | 7w | 7w | 7w | 7w | deliq |
| 134 | 6w, 4w | 6w, 4w | 6w | 7w | 7w | 7w | 7w | 7w | 7w | deliq |
| 179 | 4w, 6w | 4w, 6w | 6w | 7w | 7w | 7w | 7w | 7w | 7w | deliq |
| 224 | 4w, 6wt | 4w, 6wt | 6w | 7w | 7w | 7w | 7w | 7w | 7w | deliq |
| 351 | 4w | 4w | 6w | 7w | 7w | 7w | 7w | 7w | 7w | deliq |
| 686 | 4w | 4w | 6w | 7w | 7w | 7w | 7w | 7w | 7w | deliq |
| 1143 | 4w | 4w | 6w | 7w | 7w | 7w | 7w | 7w | 7w | deliq |
| 1979 | 4w | 4w | 4w, 6w | 7w | 7w | 7w | 7w | 7w | 7w | deliq |
| T = 5°C | | | | | | | | | | |
| | LiBr | LiCl | MgCl ₂ | Mg(NO ₃) ₂ | NaBr | KI | NaCl | KCl | KNO ₃ | H ₂ O |
| RH | 7.4 | 11.3 | 33.6 | 58.9 | 63.5 | 73.3 | 75.7 | 87.7 | 96.3 | 100 |
| Time (h) | | | | | | | | | | |
| 18 | 7w | 7w | 7w | 7w | 7w | 7w | 7w | 7w | 7w | 7w |
| 37 | 7w | 7w | 7w | 7w | 7w | 7w | 7w | 7w | 7w | 7w |
| 107 | 6w, 7w | 7w, 6w | 7w | 7w | 7w | 7w | 7w | 7w | 7w | 7w |
| 207 | 6w, 7w | 6w, 7w | 7w | 7w | 7w | 7w | 7w | 7w | 7w | deliq |
| 321 | 6w | 6w | 7w | 7w | 7w | 7w | 7w | 7w | 7w | deliq |
| 631 | 6w | 6w | 7w | 7w | 7w | 7w | 7w | 7w | 7w, deliq | 7w, deliq |
| 816 | 6w | 6w | 7w | 7w | 7w | 7w | 7w | 7w | 7w, deliq | 7w, deliq |
| 959 | 6w | 6w | 7w | 7w | 7w | 7w | 7w | 7w | 7w, deliq | 7w, deliq |
| 1270 | 6w | 6w | 7w | 7w | 7w | 7w | 7w | 7w | 7w, deliq | 7w, deliq |
| 2157 | 6w, Amt | 6w, 4w | 7w | 7w | 7w | 7w | 7w | 7w | 7w, deliq | 7w, deliq |
| 3044 | 6w, 4w | 6w, 4w | 7w | 7w | | | | | | |
| 8587 | 4w, 6wt | 4w, 6w | 6w, 7w | 7w | 7w | 7w | 7w | 7w | deliq | deliq |
| 12802 | 4w, 6wt | 4w, 6w | 7w | | | | | | | |
| 18629 | 4w | 4w, 6w | 7w | | | | | | | |

^a7w, epsomite; 6w, hexahydrate; 5w, pentahydrate; 4w, starkeyite; 3w, MgSO₄·3H₂O; 2w, sanderite; 1w, LH-1w; Am, amorphous Mg-sulfates; deliq, deliquescence; (6w, 7w), larger quantity of 6w than 7w; 6wt, trace amount of 6w; (7w, deliq), wet crystals. Bolded values are experiments that have not reached equilibrium.

2.2. Hydration and Dehydration of Starkeyite (MgSO₄·4H₂O)

[21] The hydration and dehydration experiments of starkeyite (4w, MgSO₄·4H₂O) at 50°C, 21°C, and 5°C ran for 972, 909, and 18629 h, respectively. The gravimetric measurements (Figure 3) suggest that equilibrium was reached in all experiments. The experiment at 21°C in the Mg(NO₃)₂ buffer (Figure 3, 21°C) shows a slower mass increase compared to those in NaBr and KI buffers, whereas three Raman measurements on the final product of this system were all pure 7w (Table 3), thus confirming the equilibrium suggested by *Chou and Seal* [2007].

[22] The last rows of three temperature sections in Table 3 show a similar pattern as in Table 2; that is, the final phases at high RH (>50%, 19 experiments), 7w, 6w, or deliq, were all consistent with the previously determined phase boundaries [*Chou and Seal*, 2003]. On the other hand, the final phases at lower RH (<50%) were all 4w.

[23] The straightforward phase transition pathways shown in Table 3 are significant for understanding 4w stability. At low RH(s), 4w remained unchanged during the entire dehydration process at 50°C, 21°C and 5°C. As discussed in section 2.1, the stable substructural units in 4w structure, the four-member rings, raised the activation energy

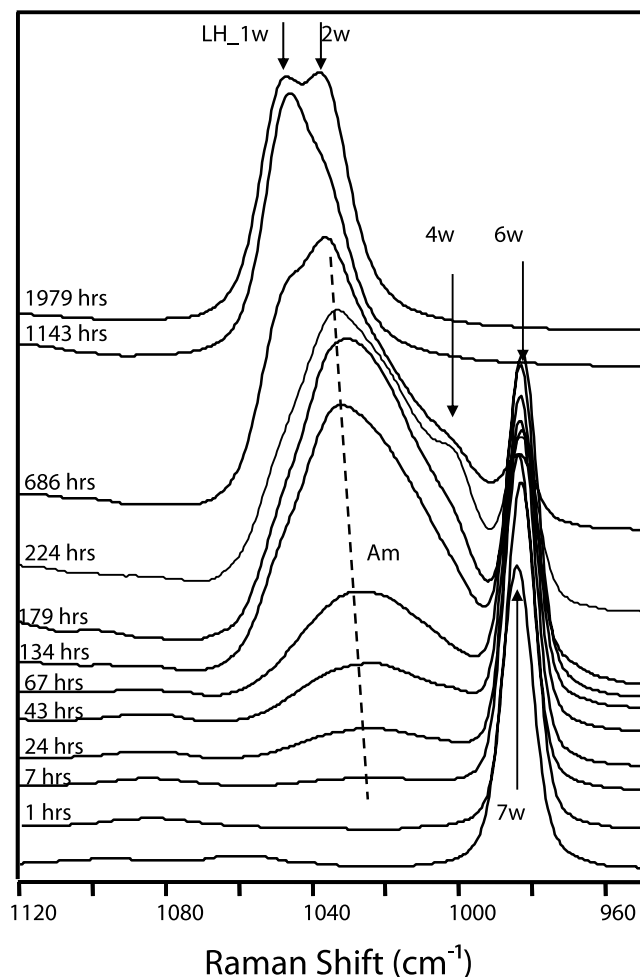


Figure 2. Pathways of forming monohydrate during dehydration (1979 h) of epsomite at 50°C and 5.5% RH from 7w → 6w → Am → Am + 4W → Am + LH-1w + 2w → LH-1w + 2w.

for phase transformation. Therefore, 4w appeared very stable at low RH (6–7%) and middle to low temperatures ($\leq 50^\circ\text{C}$). At high RH(s), 4w converted directly to 6w, to 7w, and to deliquescence (Table 3). No 5w was observed during the hydration process of 4w.

[24] We note that 1w was not formed during the dehydration of 4w at 50°C in the LiCl buffer (11% RH, Table 3) but was formed during the dehydration of 7w under the same RH-T conditions (Table 2, 50°C 11% RH). Apparently, Am was not formed during the dehydration of 4w, but was formed during the dehydration of 7w, based on two observations: (1) Am was only observed to form from 7w and 6w, but not from 4w [Wang et al., 2006c], and (2) a mixture of 1w and 2w was formed, through an intermediate Am phase as a pathway, during the dehydration of 7w at 50°C in the LiBr buffer (6% RH, Table 2). Therefore, Am must have formed during the dehydration of 7w at 50°C and 11% RH (LiCl buffer), and have served as the pathway to form the 1w + 2w + 4w mixture (Table 2). The reason for the lack of detection of Am in that experiment (Table 2) is the low Raman cross section of an amorphous phase, which is normally about 1–2

orders of magnitude lower than that of a crystalline phase of the same composition [White, 1974].

[25] It is remarkable that the dehydration processes for both 7w and 4w would all reach 4w as the equilibrium phase at low RH ($< 50\%$ RH) and middle to low temperatures ($\leq 50^\circ\text{C}$). The 1w phase only appeared in the systems where Am was first produced.

2.3. Hydration of Mg-Sulfate Monohydrate ($\text{MgSO}_4 \cdot \text{H}_2\text{O}$)

[26] The hydration of Mg-sulfate monohydrate (1w, $\text{MgSO}_4 \cdot \text{H}_2\text{O}$) at 50°C, 21°C, and 5°C ran for 2553, 2553, and 17616 h, respectively. The gravimetric measurement

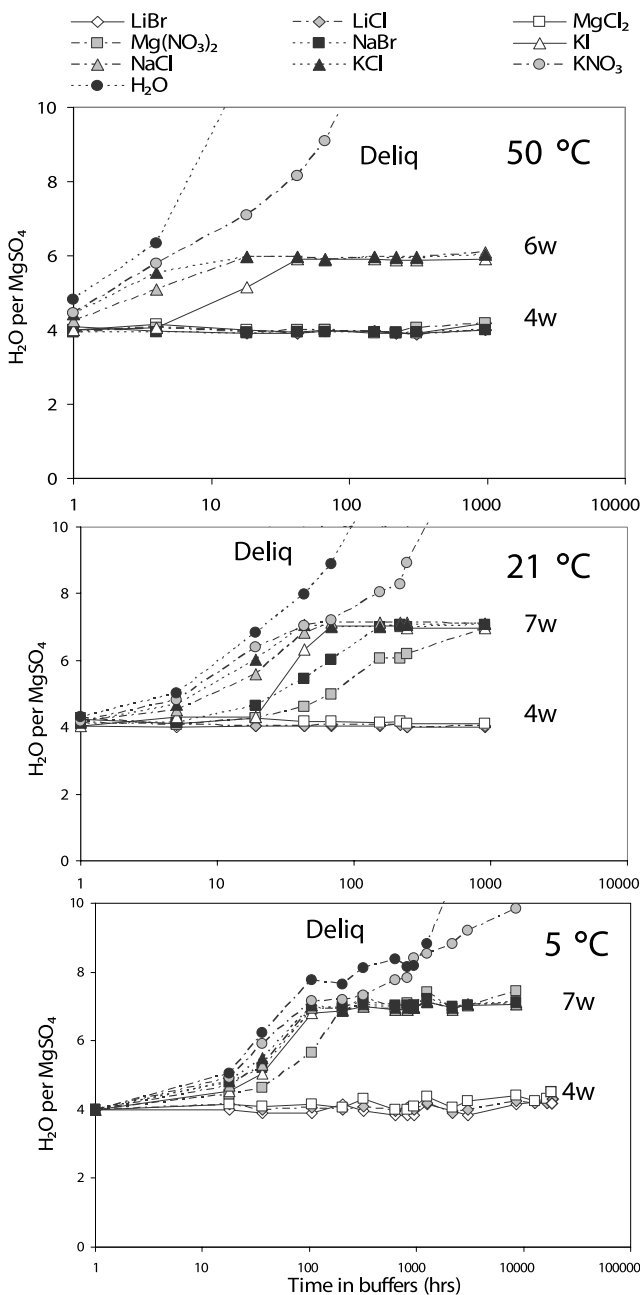


Figure 3. Gravimetric measurement results (water molecule per MgSO_4) during dehydration and rehydration of starkeyite at 50°C, 21°C, and 5°C.

Table 3. Phase Transition Pathways of Starkeyite Dehydration and Rehydration at 50°C, 21°C, and 5°C in 10 Humidity Buffers Based on Raman Spectra of the Samples

| | | T = 50°C | | | | | | | | | |
|----------|--|----------|---------|-------------------|-----------------------------------|---------|------------|--------|------------|------------------|------------------|
| | | LiBr | LiCl | MgCl ₂ | Mg(NO ₃) ₂ | NaBr | KI | NaCl | KCl | KNO ₃ | H ₂ O |
| RH | | 5.5 | 11.1 | 30.5 | 45.4 | 50.9 | 64.5 | 74.4 | 81.2 | 84.8 | 100.0 |
| Time (h) | | | | | | | | | | | |
| 1 | | 4w | 4w | 4w | 4w, 6wt | 4w, 6wt | 4w, 6wt | 4w, 6w | 4w, 6w | 4w, 6w | 6w, 4w |
| 4 | | 4w | 4w | 4w | 4w, 6wt | 4w, 6wt | 4w, 6w | 6w, 4w | 6w, 4w | 6w | 6w |
| 18 | | 4w | 4w | 4w | 4w, 6wt | 4w, 6wt | 6w, 4w | 6w | 6w | 6w, deliq | 6w, deliq |
| 42 | | 4w | 4w | 4w | 4w | 4w | 6w | 6w | 6w | 6w, deliq | deliq |
| 67 | | 4w | 4w | 4w | 4w | 4w, 6wt | 6w | 6w | 6w | 6w, deliq | deliq |
| 154 | | 4w | 4w | 4w | 4w, 6wt | 4w, 6wt | 6w | 6w | 6w | 6w, deliq | deliq |
| 218 | | 4w | 4w | 4w | 4w | 4w | 6w | 6w | 6w | 6w, deliq | deliq |
| 307 | | 4w | 4w | 4w | 4w | 4w | 6w | 6w | 6w | deliq | deliq |
| 972 | | 4w | 4w | 4w | 4w | 4w | 6w | 6w | 6w | deliq | deliq |
| | | T = 21°C | | | | | | | | | |
| | | LiBr | LiCl | MgCl ₂ | Mg(NO ₃) ₂ | NaBr | KI | NaCl | KCl | KNO ₃ | H ₂ O |
| RH | | 6.6 | 11.3 | 33.0 | 54.1 | 58.8 | 69.7 | 75.4 | 85.0 | 94.4 | 100.0 |
| Time (h) | | | | | | | | | | | |
| 1 | | 4w | 4w | 4w | 4w | 4w | 4w, 6w | 4w, 6w | 4w, 6w | 4w, 6w | 4w, 6w |
| 5 | | 4w | 4w | 4w | 4w | 4w, 6wt | 4w, 6w | 4w, 6w | 6w, 4w | 6w, 4w | 6w, 4w |
| 19 | | 4w | 4w | 4w | 4w, 6w | 4w, 6w | 6w, 4w | 6w, 4w | 6w | 6w | 7w |
| 43 | | 4w | 4w | 4w | 6w, 4w | 6w, 4w | 6w | 7w | 7w | 7w | 7w, deliq |
| 68 | | 4w | 4w | 4w | 6w, 4w | 6w, 4w | 7w | 7w | 7w | 7w | 7w, deliq |
| 156 | | 4w | 4w | 4w | 6w | 7w | 7w | 7w, 6w | 7w | 7w | 7w, deliq |
| 220 | | 4w | 4w | 4w | 6w | 7w | 7w | 7w | 7w | 7w, deliq | deliq |
| 244 | | 4w | 4w | 4w | 6w | 7w | 7w | 7w | 7w | 7w, deliq | deliq |
| 909 | | 4w | 4w | 4w | 7w | 7w | 7w | 7w | 7w | deliq | deliq |
| | | T = 5°C | | | | | | | | | |
| | | LiBr | LiCl | MgCl ₂ | Mg(NO ₃) ₂ | NaBr | KI | NaCl | KCl | KNO ₃ | H ₂ O |
| RH | | 7.4 | 11.3 | 33.6 | 58.9 | 63.5 | 73.3 | 75.7 | 87.7 | 96.3 | 100 |
| Time (h) | | | | | | | | | | | |
| 18 | | 4w | 4w, 6wt | 4w | 4w, 6w | 4w, 6w | 4w, 6w | 4w, 6w | 4w, 6w | 4w, 6w | 4w, 6w |
| 37 | | 4w | 4w | 4w | 4w, 6w | 4w, 6w | 4w, 6w, 7w | 4w, 6w | 6w, 7w, 4w | 6w, 7w, 4w | 6w, 7w, 4w |
| 107 | | 4w | 4w, 6wt | 4w | 6w, 7w, 4w | 7w, 4wt | 7w, 4wt | 7w | 7w | 7w | 7w |
| 207 | | 4w | 4w, 6wt | 4w | 7w, 4wt | 7w | 7w | 7w | 7w | 7w | 7w |
| 321 | | 4w | 4w | 4w | 7w | 7w | 7w | 7w | 7w | 7w | 7w |
| 631 | | 4w | 4w | 4w, 6w | 7w | 7w | 7w | 7w | 7w | 7w | 7w |
| 816 | | 4w | 4w, 6wt | 4w, 6wt | 7w | 7w | 7w | 7w | 7w | 7w | 7w |
| 959 | | 4w | 4w | 4w | 7w | 7w | 7w | 7w | 7w | 7w | 7w |
| 1270 | | 4w | 4w | 4w | 7w | 7w | 7w | 7w | 7w | 7w | 7w |
| 2157 | | 4w | 4w, 6wt | 4w, 6wt | 7w | 7w | 7w | 7w | 7w | 7w | 7w |
| 3044 | | 4w | 4w | 4w | 7w | 7w | 7w | 7w | 7w | 7w | 7w |
| 8587 | | 4w | 4w | 4w, 6wt | 7w | 7w | 7w | 7w | 7w | 7w, deliq | deliq |
| 12802 | | 4w | 4w | 4w, 6wt | 7w | 7w | 7w | 7w | 7w | 7w, deliq | deliq |
| 18629 | | 4w | 4w | 4w | 7w | 7w | 7w | 7w | 7w | 7w, deliq | deliq |

results (Figure 4) show that equilibrium was reached in most experiments, except one (at 21°C in the Mg(NO₃)₂ buffer). Table 4 lists the phases identified by Raman measurements at the intermediate and end stages of processes under different RH-T conditions.

[27] The last rows of three temperature sections in Table 4 show that the end products from the hydration of 1w at high RH (>50%) were consistent with the previously determined phase boundaries [Chou and Seal, 2003]; that is, 1w converts to 6w, to 7w, or to deliquescence. It is worth noting that a trace amount of 2w, MgSO₄·3H₂O (3w), and 5w occurred at a few intermediate stages under low-and-middle RH, whereas 4w was not observed at the midstages in any experiment.

[28] At low RH (≤50%), the major phase in the final products of all eleven experiments at three temperatures was 1w, thus consistent in general with Chou and Seal [2003]. Nevertheless, minor variations in Raman peak positions were observed in the midproducts and end products of the

experiments at mid-RH(s), marked as 1w_{mix}, or MH-1w in Table 4. That peak position shift was later determined to be an indication of a phase transition between two polymorphs of Mg-sulfate monohydrate, LH-1w and MH-1w. This phenomenon is discussed in section 3.2.

[29] The final phase of the system at 50°C in KI buffer (64% RH) was a mixture of 6w and MH-1w (upper spectrum in Figure 5), while the gravimetric measurement (Figure 4) suggests that equilibrium was reached after 2553 h. This set of RH-T values fell right on the 1w–6w phase boundary proposed by Chou and Seal [2003] on the basis of experimental data and a calculation of the enthalpy of reaction. Thus, the identification of coexisting MH-1w and 6w in our experiment confirms the location of this important phase boundary.

[30] The experiment at 21°C in the Mg(NO₃)₂ buffer did not reach equilibrium (Figure 4, 21°C). The end product after 2554 h was a mixture of 6w and 1w_{mix} (Table 4). The

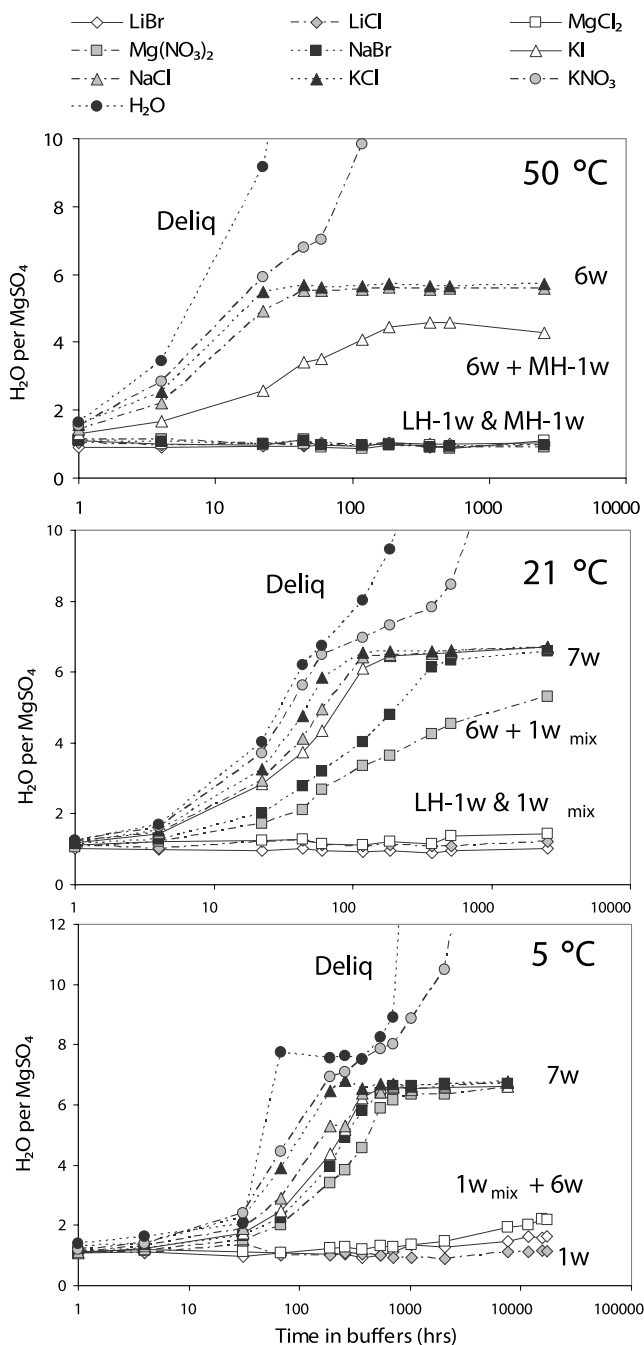


Figure 4. Gravimetric measurement results (water molecule per MgSO_4) during rehydration of monohydrate Mg-sulfate at 50°C , 21°C , and 5°C .

slope of the mass variation line for this experiment in Figure 4 suggests that a total conversion from 1w to 7w may take 11.5 years to accomplish under these RH-T conditions in our laboratory.

[31] In the system at 5°C in the MgCl_2 buffer (34% RH), part of the original 1w powder was hydrated to 6w (Table 4). The lower spectrum in Figure 5 shows a peak position shift upward from the MH-1w peak in the upper spectrum, suggesting a mixture of MH-1w and LH-1w (marked as $1w_{\text{mix}}$). The coexistence of $1w_{\text{mix}} + 6w$ lasted more than 734 days (17616 h) at 5°C and 34% RH (Table 4). The

existence of 6w in this sample was also evidenced by a mass increase of the final product to an average of 2 water molecules per MgSO_4 (Figure 4, 5°C). This set of RH-T values is located within the kieserite stability field on the left side of the 1w–7w phase boundary suggested by *Chou and Seal* [2003, 2007]. The phase transition pathway of this experiment (Table 4, 5°C and 34% RH; i.e., $1w \rightarrow 1w + 2w + 3w \rightarrow 1w + 6w$) suggest the hydration of 1w actually occurred.

[32] Comparing Tables 2 and 3 with Table 4, we observe that when the starting phase is 1w, it remains as 1w under middle to low RH levels in the temperature range $5\text{--}50^\circ\text{C}$. At higher RH, it converts to 7w and 6w, but not 4w. The hydration products of 1w match generally with the 1w–6w phase boundary suggested by *Chou and Seal* [2003, 2007], but those from reverse processes (i.e., the dehydration of 7w, 6w, and 4w) do not match. In other words, the reverse phase transitions from 7w, 6w, and 4w to 1w do not occur naturally at $T \leq 50^\circ\text{C}$, regardless of the extremely low RH buffers that we employed. The only two exceptions were found in the dehydration process of 7w at 50°C under extremely dry conditions (6% RH and 11% RH), through an intermediate amorphous Mg-sulfate (Figure 2; see detailed discussion in section 3.1). These two experiments eventually produced a mixture of 1w and 2w (Figure 2).

[33] It is worth noting that the direct conversion from 7w to 1w is possible at temperatures much higher than the current Martian surface temperatures. We have observed a partial conversion of that sort at 75°C and a total conversion at 90°C in 1–2 days.

2.4. Hydration and Dehydration of an Amorphous Mg-Sulfate ($\text{MgSO}_4 \cdot 2\text{H}_2\text{O}$)

[34] The hydration and dehydration of an amorphous Mg-sulfate ($\text{MgSO}_4 \cdot 2\text{H}_2\text{O}$ in our experiments) at 50°C , 21°C , and 5°C were run for 823, 1309, and 17616 h, respectively. Two additional experiments in LiI and NaI buffers at 21°C (18% and 39% RH) were run over 2534 h. The gravimetric measurement results (Figure 6) suggest that equilibrium was reached in all systems, except the one in the MgCl_2 buffer at 5°C .

[35] Within the high RH range ($>50\%$), the equilibrated phases (Table 5) were consistent with the previously determined phase boundaries [*Chou and Seal*, 2003] with two exceptions (bold in Table 5): (1) a mixture of 6w plus deliq was found in the system at 50°C in the KCl buffer (6w stability field); and (2) a mixture of 6w plus 7w was found in the system at 50°C in the KI buffer, right on the 6w–1w phase boundary. The common characteristic of these abnormal results was the presence of phases with a higher hydration degree (liquid and 7w), which suggests that the irregular structural framework in amorphous Mg-sulfate may have facilitated the rehydration process.

[36] Within the low RH range ($\leq 50\%$), we observed (1) amorphous Mg-sulfate was stable at low relative humidity (RH $< 20\%$) for long durations (2534–17616 h); (2) 1w + 2w mixtures were formed from amorphous Mg-sulfates at 31% RH and 50°C (Table 5), confirming a similar observation in the dehydration experiment of 7w (Figure 2 and Table 2); (3) 4w, not 1w, was the final and stable phase at mid-RH (34–51% RH in MgCl_2 , NaI, $\text{Mg}(\text{NO}_3)_2$, and NaBr

Table 4. Phase Transition Pathways of Monohydrated Mg-Sulfates Rehydration at 50°C, 21°C, and 5°C in 10 Humidity Buffers Based on Raman Spectra of the Samples^a

| T = 50°C | | | | | | | | | | |
|----------|--------------|---------|-----------------------------|-----------------------------------|------------------------------|-----------------------|------------|---------|------------------|------------------|
| | LiBr | LiCl | MgCl ₂ | Mg(NO ₃) ₂ | NaBr | KI | NaCl | KCl | KNO ₃ | H ₂ O |
| RH | 5.5 | 11.1 | 30.5 | 45.4 | 50.9 | 64.5 | 74.4 | 81.2 | 84.8 | 100.0 |
| Time (h) | | | | | | | | | | |
| 1 | 1w | 1w | 1w, 6wt | 1w, 6wt | 1w, 6w | 1w, 6w | 1w, 6w | 1w, 6w | 1w, 6w | 6w, 1w |
| 4 | 1w | 1w | 1w, 6wt | 1w, 6wt, 5w | 1w, 6wt, 5wt | 6w, 1w | 6w, 1w | 6w, 1w | 6w, 1w | 6w, 1w |
| 23 | 1w | 1w | 1w _{mix} | 1w, 5w | 1w, 6wt, 5wt | 6w, 1w | 6w, 1w | 6w | 6w | 6w |
| 44 | 1w | 1w | 1w _{mix} | 1w, 5w | 1w, 5wt | 6w, 1w _{mix} | 6w | 6w | 6w | deliq |
| 60 | 1w | 1w | 1w _{mix} | 1w _{mix} , 6wt | 1w _{mix} , 6wt, 5wt | 6w, 1w _{mix} | 6w | 6w | deliq | deliq |
| 118 | 1w, 5wt | 1w | 1w _{mix} | 1w _{mix} , 6wt | 1w _{mix} | 6w, MH-1w | 6w | 6w | deliq | deliq |
| 187 | 1w | 1w | 1w _{mix} | 1w _{mix} , 6wt | 1w _{mix} | 6w, MH-1w | 6w | 6w | deliq | deliq |
| 370 | 1w | 1w | 1w _{mix} | 1w _{mix} , 6wt | 1w _{mix} | 6w, MH-1w | 6w | 6w | deliq | deliq |
| 514 | 1w | 1w | 1w _{mix} | 1w _{mix} x | MH-1w, 5wt | 6w, MH-1w | 6w | 6w | deliq | deliq |
| 2554 | 1w | 1w | 1w _{mix} | 1w _{mix} | MH-1w | 6w, MH-1w | 6w | 6w | deliq | deliq |
| T = 21°C | | | | | | | | | | |
| | LiBr | LiCl | MgCl ₂ | Mg(NO ₃) ₂ | NaBr | KI | NaCl | KCl | KNO ₃ | H ₂ O |
| RH | 6.6 | 11.3 | 33.0 | 54.1 | 58.8 | 69.7 | 75.4 | 85.0 | 94.4 | 100.0 |
| Time (h) | | | | | | | | | | |
| 1 | 1w | 1w | 1w, | 1w, 6wt | 1w, 6wt | 1w, 6w | 1w, 6w | 1w, 6w | 1w, 6w | 1w, 6w |
| 4 | 1w | 1w | 1w, | 1w, 6w | 1w, 6w | 1w, 6w | 1w, 6w | 1w, 6w | 1w, 6w | 6w, 1w |
| 23 | 1w, 6wt | 1w, 6wt | 1w, 6wt | 1w, 6w | 1w, 6w | 6w, 1w | 6w, 1w | 6w, 1w | 6w, 1w | 6w, 1w |
| 44 | 1w, 6wt | 1w, 6wt | 1w, 6wt, 5wt | 6w, 1w | 6w, 1w | 6w, 1wt | 6w, 1wt | 6w, 1wt | 6w | 6w, 7w |
| 60 | 1w, 6wt | 1w, 6wt | 1w, 6wt, 5wt | 6w, 1w | 6w, 1w | 6w | 6w, 1wt | 6w, 7w | 7w | 7w |
| 118 | 1w, 6wt | 1w, 6wt | 1w, 6wt, 5wt | 6w, 1w | 6w, 1w | 6w, 7w | 7w | 7w, 6w | 7w | deliq |
| 187 | 1w, 6wt | 1w, 6wt | 1w, 6wt, 5wt, | 6w, 1w | 6w, 1wt | 7w | 7w | 7w, 6w | 7w | deliq |
| 370 | 1w | 1w | 1w, 6wt, 5wt, | 6w, 1w | 6w, 1wt | 6w, 7w | 7w | 7w | 7w | deliq |
| 514 | 1w | 1w | 1w, 6wt, 5wt, | 6w, 1w _{mix} | 6w, 7w | 6w, 7w | 7w | 7w | 7w | deliq |
| 2554 | 1w | 1w | 1w _{mix} | 6w, 1w_{mix} | 7w | 7w | 7w | 7w | 7w | deliq |
| T = 5°C | | | | | | | | | | |
| | LiBr | LiCl | MgCl ₂ | Mg(NO ₃) ₂ | NaBr | KI | NaCl | KCl | KNO ₃ | H ₂ O |
| RH | 7.4 | 11.3 | 33.6 | 58.9 | 63.5 | 73.3 | 75.7 | 87.7 | 96.3 | 100 |
| Time (h) | | | | | | | | | | |
| 1 | 1w, 2wt, 3wt | 1w, 3wt | 1w, 3wt | 1w, 3wt | 1w, 3wt | 1w, 2w, 3wt, 6wt | 1w, 3wt | 1w, 6wt | 1w, 6wt | 1w, 6wt |
| 4 | 1w, 3wt | 1w, 3wt | 1w, 3wt | 1w | 1w, 6wt | 1w, 6wt | 1w, 6w, 7w | 1w, 6wt | 1w, 6w | 6w, 1w |
| 31 | 1w, 3wt | 1w, 3wt | 1w, 2wt, 6w | 6w, 1w | 6w, 1w | 1w, 6w | 6w, 1w | 6w, 1w | 6w, 1w | 6w, 1w |
| 68 | 1w, 3wt | 1w, 3wt | 1w, 3wt, 6wt | 6w, 1w, 3wt | 6w, 1w, 3wt | 6w, 1w, 3wt | 6w, 1w | 6w, 1w | 6w, 7w, 1w | 7w |
| 190 | 1w, 3wt, 6wt | 1w, 3wt | 1w, 3wt, 6wt | 6w, 1w | 6w, 1w | 6w, 1w | 6w, 1w | 7w | 7w | 7w |
| 256 | 1w, 3wt, 6wt | 1w, 3wt | 1w, 3wt, 6wt | 6w, 1w | 6w, 7w, 1w | 6w, 7w, 1w | 6w, 7w | 7w | 7w | 7w |
| 371 | 1w, 2wt | 1w | 1w, 6w | 6w, 7w, 1w | 6w, 7w, 1w | 7w | 7w, 6w | 7w | 7w | 7w, deliq |
| 536 | 1w | 1w | 1w, 6w | 6w, 7w | 6w, 7w | 7w | 7w, 6w | 7w | 7w | 7w, deliq |
| 699 | 1w | 1w | 1w _{mix} , 6w | 6w, 7w | 6w, 7w | 6w, 7w | 6w, 7w | 6w, 7w | 7w, deliq | 7w, deliq |
| 1028 | 1w | 1w | 1w _{mix} , 6w | 7w | 7w | 7w | 7w | 7w | 7w, deliq | 7w, deliq |
| 2055 | 1w | 1w | 1w _{mix} , 6w | 7w | | | | | | |
| 7574 | 1w | 1w, 2wt | 1w _{mix} , 6w | 7w | 7w | 7w | 7w | 7w | deliq | deliq |
| 11790 | 1w | 1w | 1w _{mix} , 6w | | | | | | | |
| 17616 | 1w | 1w | 1w_{mix}, 6w | | | | | | | |

^aMonohydrated Mg-sulfates used as starting phase of this set of experiments are LH-1w, 1w, LH-1w; 1w_{mix}, mixture of LH-1w and MH-1w. The difference between MH-1w and LH-1w is discussed in section 3.2.

buffers) and all Ts (5°C to 50°C) when amorphous Mg-sulfate was the starting phase (Table 5).

[37] We note that in Tables 4 and 5 and Figure 6, 6w appears at 5°C in the MgCl₂ buffer (34% RH), which indicates that the hydration processes occurred under these conditions when 1w and Am were the starting phases. The coexistence of 4w + 5w + 6w, or 1w_{mix} + 6w, lasted nearly 24 months in these experiments. Although equilibrium was not reached yet (Figures 4 and 6), the development tendencies clearly indicate the increase of hydration states from the starting phases (1w and Am). These two experimental observations apparently suggest that the location of the 1w–7w phase boundary [cf. *Chou and Seal*, 2003, 2007] in this RH-T region should be moved toward lower RH's, to pass the point at 5°C and 34% RH. Given that the 1w–7w

boundary suggested by *Chou and Seal* [2003, 2007] would pass through 35.6% RH at 5°C, and that the RH control accuracy in our experimental setting is about ±1%, the difference between our experiments and their boundary determination is very minor. Thus, our experimental observations actually confirm the general location of the 1w–7w boundary at 5°C, similar to the confirmation provided for the general location of the 1w–6w boundary at 50°C.

[38] Table 5 lists the phase transition pathways of the hydration and dehydration of amorphous Mg-sulfates. At high RH (>50%), a general hydration trend of amorphous Mg-sulfates is →4w → 6w → 7w → Deliq. Of significance is the difference in the hydration pathway of amorphous Mg-sulfate from that of 1w; the latter converts directly to 6w without going through 4w (Table 4).

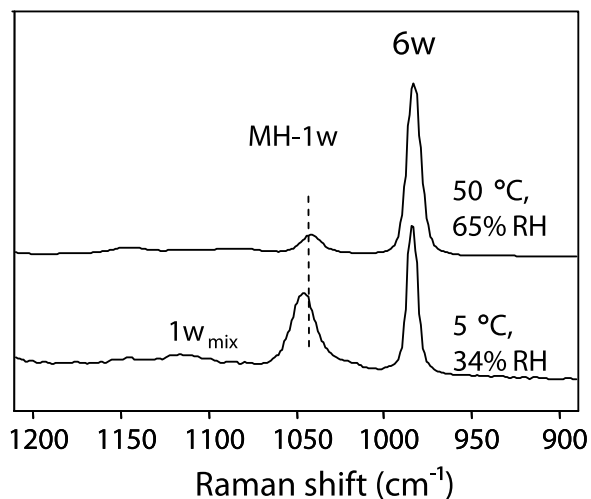


Figure 5. Raman spectra obtained from the products of rehydration of $\text{MgSO}_4 \cdot \text{H}_2\text{O}$ that confirmed the locations of two phase boundaries: (1) MH-1w + 6w at 50°C and 64.5% RH at 1w–6w phase boundary. (2) $1w_{\text{mix}}$ + 6w at 5°C and 33.6% RH near 1w–7w phase boundary.

[39] At low RH ($\leq 20\%$), amorphous Mg-sulfates remain amorphous, but the ν_1 Raman peak position shifts to lower wave number upon hydration (Figure 7). At mid-RH (31–34% RH in the MgCl_2 buffer of three Ts), all crystalline hydration states of Mg-sulfates (including 1w, 2w, 3w, 4w, 5w, 6w, and 7w, but not 11w, which is not stable above 2°C) appear among the intermediate products of Am rehydration experiments (Figure 8 and Table 5). Apparently, the irregular structural framework of the amorphous Mg-sulfates reduces phase transition barriers and facilitates the formation of a variety of crystalline Mg-sulfates.

2.5. Dehydration of Epsomite When Mixed With Ca-Sulfates, Fe-Sulfates, Fe-Oxide, and Fe-Hydroxide

[40] Mixtures of Ca- and Mg-sulfates were used in the first set of mixing experiments. Six samples were prepared by mixing epsomite (7w, powder size $< 75 \mu\text{m}$) with anhydrite (CaSO_4), bassanite ($\text{CaSO}_4 \cdot 0.5\text{H}_2\text{O}$), and gypsum ($\text{CaSO}_4 \cdot 2\text{H}_2\text{O}$) powder of similar grain size at two molar ratios: about 8:2 and 4:6 of $\text{MgSO}_4 \cdot 7\text{H}_2\text{O}$ to $\text{CaSO}_4 \cdot x\text{H}_2\text{O}$ ($x = 0, 0.5, 2$, Table 6). These mixtures were put in MgCl_2 buffers (31% RH) at 50°C for 2531 h, with systematic gravimetric and noninvasive Raman measurements made at regular time intervals. The MgCl_2 humidity buffer was chosen because it provides an RH in the midrange of the RH-T stability field of kieserite, where 1w has not been seen to form from direct dehydration of 7w (section 3.1 and Table 2). The intent of the first set of mixing experiments was to examine the effect of Ca-sulfates, with different hydration states and different proportions, on the dehydration pathway of epsomite (7w). We wanted to test if a monohydrate Mg-sulfate can be produced from epsomite (7w) when epsomite was mixed with one of the Ca-sulfates.

[41] Figure 9 shows the Raman spectra of anhydrite, bassanite, and gypsum. Figure 10 shows the characteristic Raman spectra of the known Mg-sulfates (hydrated and anhydrous, crystalline and amorphous). These spectra show

that the characteristic Raman peaks of the three Ca-sulfates do not overlap with those of the hydrates of Mg-sulfate; thus phases can be identified by visual inspection of raw Raman spectra of Mg- and Ca-sulfate mixtures.

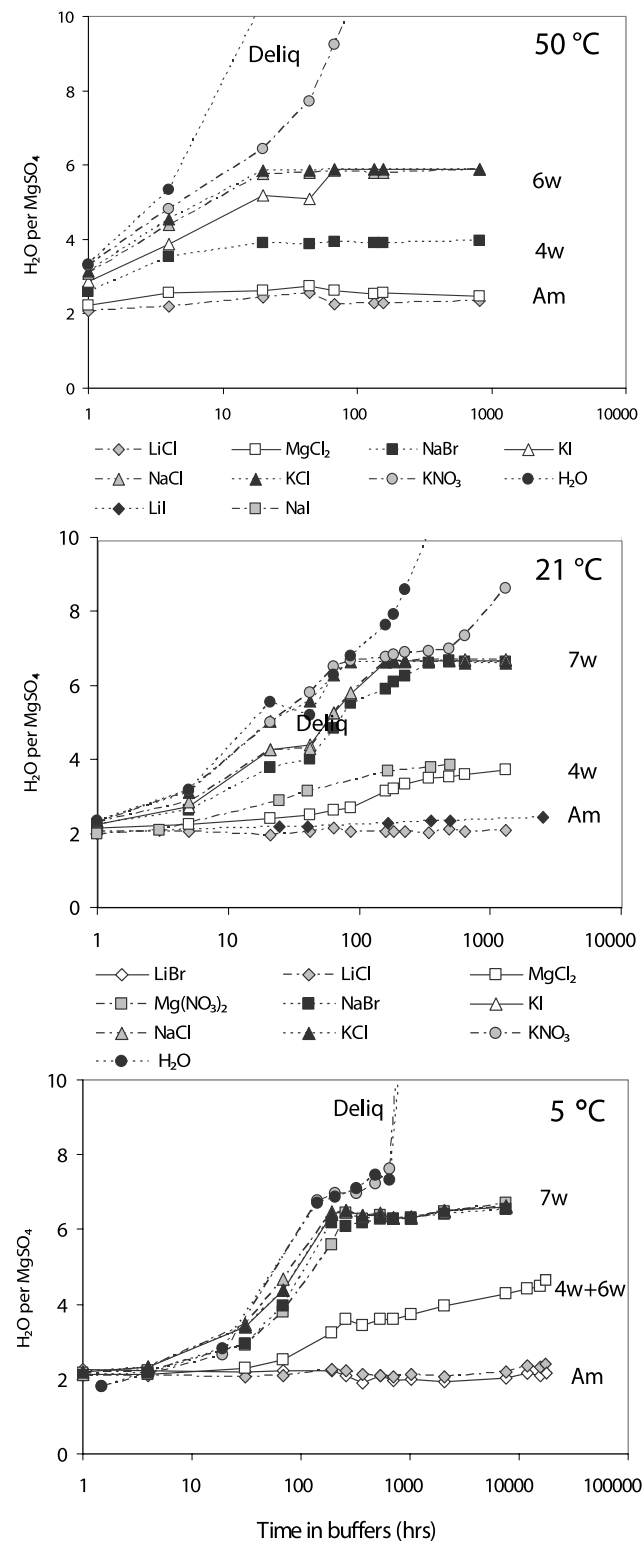


Figure 6. Gravimetric measurement results (water molecule per MgSO_4) during dehydration and rehydration of amorphous Mg-sulfate at 50°C , 21°C , and 5°C .

Table 5. Phase Transition Pathways of Am Dehydration and Rehydration at 50°C, 21°C, and 5°C in 10 Humidity Buffers Based on Raman Spectra of the Samples^a

| | | T = 50°C | | | | | | | | | |
|----------|-----------|-----------|-------------------|-------------------|-----------------------------------|--------------|------------------|------------------|------------------|---------------------|------------------|
| | | LiCl | MgCl ₂ | NaBr | KI | NaCl | KCl | KNO ₃ | H ₂ O | | |
| RH | | 11.1 | 30.5 | 50.9 | 64.5 | 74.4 | 81.2 | 84.8 | 100.0 | | |
| Time (h) | | | | | | | | | | | |
| 1 | Am | Am | Am | Am | Am | Am | Am | 4w, Am, 7w | Am, 7w, 4w | | |
| 4 | Am | Am | Am | 4w, Am | 4w, 6wt | 6w, 4w | 4w, 6w | 6w, 4w | 6w | | |
| 20 | Am | | 2w, 1w, 4w, Am | 4w, 6wt | 6w, 4w | 6w | 6w | 6w | 6w, deliq | | |
| 44 | Am | | 2w, 1w, 4wt | 4w | 6w | 6w | 6w | 6w, deliq | deliq | | |
| 68 | Am | | 2w, 1w | 4w, 6wt | 6w | 6w | 6w | 6w, deliq | deliq | | |
| 135 | Am | | 2w, 1w, 4wt | 4w | 6w | 6w | 6w | deliq | deliq | | |
| 158 | Am | | 2w, 1w | 4w | 6w | 6w | 6w | deliq | deliq | | |
| 823 | Am | | 2w, 1w | 4w | 6w, 7w | 6w | 6w, deliq | deliq | deliq | | |
| | | T = 21°C | | | | | | | | | |
| | | LiCl | LiI | MgCl ₂ | NaI | NaBr | KI | NaCl | KCl | KNO ₃ | H ₂ O |
| RH | | 11.3 | 18.4 | 33.0 | 39.4 | 58.8 | 69.7 | 75.4 | 85.0 | 94.4 | 100.0 |
| Time (h) | | | | | | | | | | | |
| 1 | Am | | | Am | | Am | Am | Am | Am | Am | Am |
| 5 | Am | Am | | Am | Am | 4w, Am, 6w | 4w, 6w, Am | 4w, Am, 6w | 6w, Am, 4w | 6w, 4w, Am | 6w, 4w, Am |
| 21 | Am | Am | | Am, 4wt | Am, 4w | 4w, Am, 6w | 4w, 6w, Am | 6w, 4w, Am | 6w, 4w | 6w, 4w | 7w, 6w |
| 43 | Am | Am | | Am, 2wt, 3wt, 4wt | Am, 4w | 6w, Am | 6w, Am | 6w, Am | 6w | 6w, 7w | 6w |
| 65 | Am | | | Am, 2wt, 4wt | | 6w, 4wt, 5wt | 6w, 4wt | 6w | 6w, 7w | 7w | 6w, 7w |
| 87 | Am | | | Am, 6w, 4wt, 2wt | | 6w, 5wt | 6w | 6w | 7w | 7w | 7w, deliq |
| 159 | Am | Am | | Am, 4w, 6w | 4w | 6w | 7w | 7w | 7w | 7w | 7w, deliq |
| 183 | Am | | | Am, 4w, 5w, 6w | | 7w, 6w | 7w | 7w | 7w | 7w, deliq | deliq |
| 225 | Am | | | Am, 4w, 5w, 6w | | 7w, 6w | 7w | 7w | 7w | 7w, deliq | deliq |
| 342 | Am | Am | | 4w, 5wt, Am | 4w | 7w, 6w | 7w | 7w, 6w | 7w | 7w, deliq | deliq |
| 486 | Am | Am | | 4w, 5wt, Am | 4w | 7w | 7w | 7w | 7w | 7w, deliq | deliq |
| 643 | Am | | | 4w | | 7w | 7w | 7w | 7w | deliq | deliq |
| 1309 | Am | | | 4w | | 7w | 7w | 7w | 7w | deliq | deliq |
| 2534 | | Am, 6w | | | 4w | | | | | | |
| | | T = 5°C | | | | | | | | | |
| | | LiBr | LiCl | MgCl ₂ | Mg(NO ₃) ₂ | NaBr | KI | NaCl | KCl | KNO ₃ | H ₂ O |
| RH | | 7.4 | 11.3 | 33.6 | 58.9 | 63.5 | 73.3 | 75.7 | 87.7 | 96.3 | 100 |
| Time (h) | | | | | | | | | | | |
| 1 | Am | Am | | Am | Am | Am | Am | Am, 6wt | Am | Am | Am |
| 4 | Am | Am | | Am | Am | Am, 4wt | Am, 7w, 4wt | Am, 7wt, 4wt | Am, 7w | | |
| 31 | Am | Am | | Am, 4w, 6wtr | 6w, Am, 4w | 6w, Am, 4w | 6w, 4w, Am | 6w, 4w, Am | 6w, 4w, Am | Am, 6w, 2w, 3w, 4wt | Am, 6w |
| 68 | Am | Am | | 4w, Am, 6w | 6w, Am, 4w | 6w, 4w, Am | 6w, 4w, Am | 6w, 4w, Am | 6w, 4wtr | | |
| 190 | Am | Am | | 4w, Am, 6w | 6w | 6w, 7w | 7w | 7w | 7w | 7w | 7w |
| 256 | Am | Am | | 6w, Am, 4w | 7w | 7w | 7w | 7w | 7w | 7w | 7w |
| 371 | Am | Am | | 4w, 7w, Am | 7w | 7w | 7w | 7w | 7w | 7w | 7w |
| 536 | Am | Am, 4w | | 4w, 7w, Am | 7w, 6w | 7w, 6w | 7w | 7w | 7w | 7w | 7w, deliq |
| 699 | Am | Am | | 4w, Am, 6w | 7w, 6w | 7w, 6w | 7w, 6w | 7w, 6w | 7w, 6w | 7w, deliq | 7w, deliq |
| 1028 | Am, 4wt | Am | | 4w, Am, 6w | 7w | 7w, 6w | 7w, 6w | 7w, 6w | 7w | 7w, deliq | 7w, deliq |
| 2055 | Am | Am | | 4w, Am, 6w | 7w | | | | | | |
| 7574 | Am | Am | | 4w, 6w, 5w | 7w | 7w | 7w | 7w | 7w, deliq | deliq | deliq |
| 11790 | Am | Am | | 4w, 6w | | | | | | | |
| 17616 | Am | Am | | 4w, 5w, 6w | | | | | | | |

^aAm, Amorphous Mg-Sulfates. The types of humidity buffers used for the experiments were indicated by the first row. Different types of buffers used for specific experiments are indicated as LiBr (7.4), LiI (18.4), and NaI (39.4). Bold values are experiments that have abnormal results or have not reached equilibrium. 1w in this table are LH-1w.

[42] We assumed that the hydration states of Ca-sulfates were unchanged in this set of experiments because the hydration/dehydration rates of Ca-sulfates are extremely slow [Hardie, 1967; Blount and Dickson, 1973; Møller, 1988]. This assumption was confirmed by our observation that no Raman peak position shifts of Ca-sulfates were seen when measuring the Mg- and Ca-sulfate mixtures at the intermediate and final stages of our mixing experiments. The gravimetric measurements indicated (not shown here) that the equilibria in all six experiments progressed toward an average of four water molecules per MgSO₄ (i.e., starkeyite).

[43] Table 6 lists the Mg-sulfates and Ca-sulfates identified by Raman measurements at the intermediate and final stages of these experiments. The first set of results is as follows:

[44] 1. When epsomite (7w) was mixed originally with bassanite and gypsum, starkeyite (4w) was the end product of epsomite dehydration. These results were basically consistent with those in a pure Mg-sulfate system (Table 2). The only difference was that pentahydrate (5w) appeared in the early stages of dehydration (Table 6), which was not observed in pure Mg-sulfate systems (Table 2).

[45] 2. When epsomite was mixed originally with anhydrite, a mixture of monohydrate Mg-sulfate (1w) and sanderite

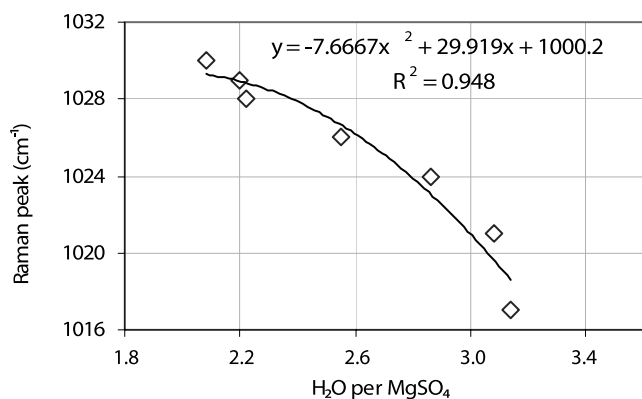


Figure 7. Raman peak position of amorphous Mg-sulfates as a function of their structural water content (water molecules per formula unit (WMPFU)).

(2w) was produced (Table 6 and Figure 11) at intermediate stages. The Mg-sulfate at equilibrium was starkeyite (4w), owing to the selection of this particular set of RH-T conditions. The details are discussed in section 3.1.

[46] Mixtures of Mg-, Fe-, and Ca-sulfates, Fe-oxide and Fe-hydroxide were used in the second set of mixing experiments. Twelve samples were prepared by mixing epsomite (7w) with melanterite ($\text{FeSO}_4 \cdot 7\text{H}_2\text{O}$), kornelite ($\text{Fe}_2(\text{SO}_4)_3 \cdot 7\text{H}_2\text{O}$), lausenite ($\text{Fe}_2(\text{SO}_4)_3 \cdot 5\text{H}_2\text{O}$), hematite (Fe_2O_3), goethite (FeOOH), and anhydrite (CaSO_4 , to repeat the first mixing experiment) at molar ratios shown in Table 7. These mixtures were put in LiCl and MgCl_2 buffers at 50°C (11% and 31% RH), with systematic gravimetric and noninvasive Raman measurements made at regular time intervals. After 2928 h dehydration, Mg-sulfate monohydrate (1w) was observed in the end products from all mixtures. Figure 12 shows the phase identification made by Raman measurements during the development of equilibrium in the epsomite and kornelite mixture at 50°C in the LiCl buffer (11% RH). The final phases at equilibrium for this experiment were monohydrated Mg-sulfate (Mg-LH-1w) and kornelite (Fe-7w). It is notable that in the repeated experiment where an epsomite and anhydrite mixture was used as starting material (at 50°C in the MgCl_2 buffer), starkeyite (4w) was observed again, but coexisting with a monohydrate Mg-sulfate. This result was in general consistent with the observation in the first set of mixing experiments (Figure 11).

3. Discussion of Five Specific Observations

[47] The emphasis of our study is to understand the pathways of forming monohydrate Mg-sulfate at a middle to low T-RH range relevant to the surface and near-surface environmental conditions on Mars. We also focus on the potential stability of Mg-sulfates with intermediate degrees of hydration and the role of amorphous Mg-sulfates in Mg-sulfate phase transitions.

3.1. Pathways of Forming Monohydrate Mg-Sulfate at Middle to Low Temperature Range

[48] On Mars, Mg-sulfate monohydrate was detected by OMEGA (Mars Express) and CRISM (MRO). Its widespread occurrences are reported within Internal Layered

Deposits of Valles Marineris (e.g., a 1.5 km thick layer at the base of the 3 km thick central mesa at Ganges Chasma [Mangold *et al.*, 2006]), within Terra Meridiani (e.g., ~1 km thickness across a several hundred km wide region [Arvidson, 2006]), and in other chaotic regions. NIR spectral matches are seen in three major absorption regions: 1.6 μm , 2.1 μm , and 2.4 μm , compared to the laboratory spectrum of a monohydrate Mg-sulfate [Arvidson *et al.*, 2005]. The monohydrate Mg-sulfate was found mostly occurring on strongly eroded, steep slopes. This observation suggests that the monohydrate Mg-sulfate was present in bedrock and was exhumed by erosion as opposed to resulting from surface interactions.

[49] Three commonly accepted formation mechanisms for Martian sulfates are (1) deposition during evaporitic process from aqueous solutions, (2) alteration of preexisting materials by groundwater/brine circulation, and (3) acid-fog alteration of igneous rocks. The geomorphic setting of these Martian monohydrate Mg-sulfate deposits favors the first two mechanisms [Mangold *et al.*, 2007]. Both mechanisms require Mg-sulfates to be deposited from S-bearing aqueous solutions. The experimental study on Mg-sulfate phase boundaries by Chou and Seal [2003, 2007] indicated that hydrated Mg-sulfate deposited from Mg-S-rich aqueous solutions should be epsomite (7w, $T < 48^\circ\text{C}$) under the current (and estimated past) average temperature range in the equatorial regions of Mars. In the polar regions of Mars, the stable Mg-sulfate hydrate should be meridianiite ($\text{MgSO}_4 \cdot 11\text{H}_2\text{O}$) [Peterson and Wang, 2006]. Therefore, the Mg-sulfate monohydrate on Mars, especially the light-toned layered

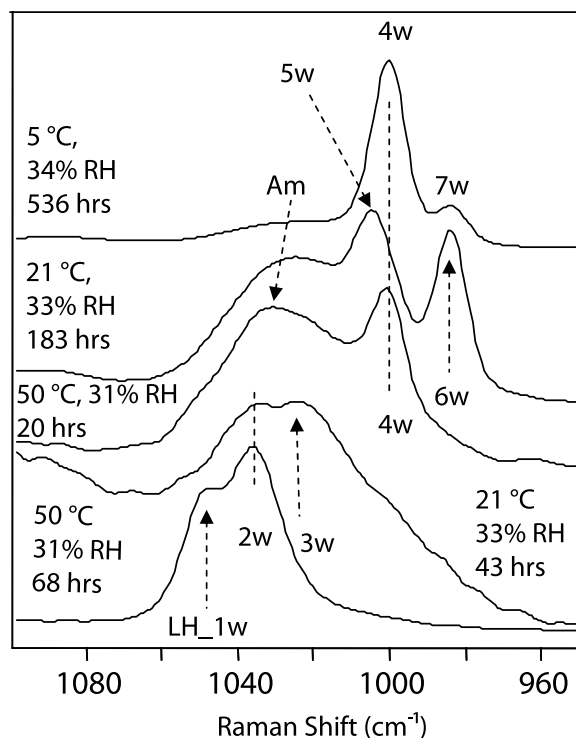


Figure 8. All crystalline Mg-sulfates (7w, 6w, 5w, 4w, 3w, 2w, and LH-1w) that appeared during dehydration and rehydration of amorphous Mg-sulfate at 50°C, 21°C, and 5°C.

Table 6. Phase Transition Pathway of the Dehydrations of Epsomite $\text{MgSO}_4 \cdot 7\text{H}_2\text{O}$ Mixed With $\text{CaSO}_4 \cdot n\text{H}_2\text{O}$ at 50°C and in MgCl_2 Buffer^a

| | Mixtures | | | | | |
|--------------|-------------------------|----------------------------|--------------------------|------------------|---------------------|------------------|
| | 7w + Anhydrite (n = 0) | | 7w + Bassanite (n = 0.5) | | 7w + Gypsum (n = 2) | |
| Molar ratios | 0.803:0.197 | 0.394:0.606 | 0.800:0.200 | 0.399:0.601 | 0.798:0.202 | 0.399:0.601 |
| Time (h) | | | | | | |
| 1 | 6w, Anh | 6w, Anh | 6w, Bas | 7w, 6w, Bas | 7w, 6w, Gyp | 6w, Gyp |
| 5 | 6w, Anh | 6w, Anh | 6w, 4w, Bas | 6w, Bas | 6w, Gyp | 6w, Gyp |
| 27 | 6w, 5w, 4w, 2w, 1w, Anh | 6w, Anh | 6w, 4w, Bas | 6w, 4w, 5w, Bas | 6w, 4w, Gyp | 6w, 4w, Gyp |
| 47 | 6w, 4w, 2w, 1w, Anh | 6w, 4w, Anh | 4w, 6wt, 5wt, Bas | 4w, 6w, 5wt, Bas | 4w, 6wt, 5wt, Gyp | 4w, 6w, 5wt, Gyp |
| 69 | 4w, 2w, 1w, 6w, Anh | 6w, 4w, 5w, 2w, 1w, Anh | 4w, 6wt, Bas | 4w, 6wt, Bas | 4w, 6w, 5wt, Gyp | 4w, 6w, Gyp |
| 91 | 4w, 2w, 1w, 6w, Anh | 6w, 4w, 5wt, 2wt, 1wt, Anh | 4w, 5wt, Bas | 4w, Bas | 4w, Gyp | 4w, 6wt, Gyp |
| 113 | 4w, 2wt, 1wt, 6wt, Anh | 4w, 6w, 2w, 1w, Anh | 4w, Bas | 4w, Bas | 4w, Gyp | 4w, 6w, Gyp |
| 184 | 4w, 6wt, 2wt, 1wt, Anh | 4w, 6wt, 2wt, 1wt, Anh | 4w, Bas | 4w, Bas | 4w, Gyp | 4w, 6wt, Gyp |
| 248 | 4w, 6w, 2w, 1w, Anh | 4w, 2wt, 1wt, Anh | 4w, Bas | 4w, Bas | 4w, Gyp | 4w, 6wt, Gyp |
| 330 | 4w, 2wt, 1wt, Anh | 4w, 6w, 2wt, 1wt, Anh | 4w, Bas | 4w, Bas | 4w, Gyp | 4w, Gyp |
| 404 | 4w, 2wt, 1wt, Anh | 4w, 2w, 1w, Anh | 4w, Bas | 4w, Bas | 4w, Gyp | 4w, Gyp |
| 587 | 4w, 5w, 2w, 1w, Anh | 4w, 6w, 2wt, 1wt, Anh | 4w, Bas | 4w, Bas | 4w, Gyp | 4w, Gyp |
| 707 | 4w, 2w, 1w, Anh | 4w, 2wt, 1wt, Anh | 4w, Bas | 4w, Bas | 4w, Gyp | 4w, Gyp |
| 2531 | 4w, 6wt, 2wt, 1wt, Anh | 4w, 6wt, Anh | 4w, Bas | 4w, Bas | 4w, Gyp | 4w, Gyp |

^aAnh, CaSO_4 ; Bas, $\text{CaSO}_4 \cdot 1/2\text{H}_2\text{O}$; Gyp, $\text{CaSO}_4 \cdot 2\text{H}_2\text{O}$; 1w, LH-1w. RH is 30.5%

deposits in the Valles Marineris, should have originated from the dehydration of epsomite (7w).

[50] The experimental results described in this paper, however, suggest that Mg-sulfate monohydrate cannot be formed directly from dehydration of epsomite (7w) at intermediate to low temperatures (5°C to 50°C). Mg-sulfate monohydrate can be formed in the laboratory when epsomite (7w) is heated at significantly elevated temperatures ($>75^\circ\text{C}$); however, this is an unrealistic temperature range for either current or past Martian surface temperatures (except perhaps

at localized hydrothermal sites, or beneath several kilometers of burial depths). In other words, the 6w–1w and 7w–1w phase boundaries in the temperature range 5°C to 50°C [Chou and Seal, 2003] is not obeyed by the dehydration process of epsomite (Table 4). In our experiments in middle to low T-RH range (5°C to 50°C , $\leq 50\%$ RH), the direct dehydration product of 7w and 6w is 4w by slow dehydration (Table 2) and Am by rapid dehydration [Vaniman et al., 2004; Wang et al., 2006c]. In addition, we find that 4w and Am are extremely stable at low RH within our experimental T range

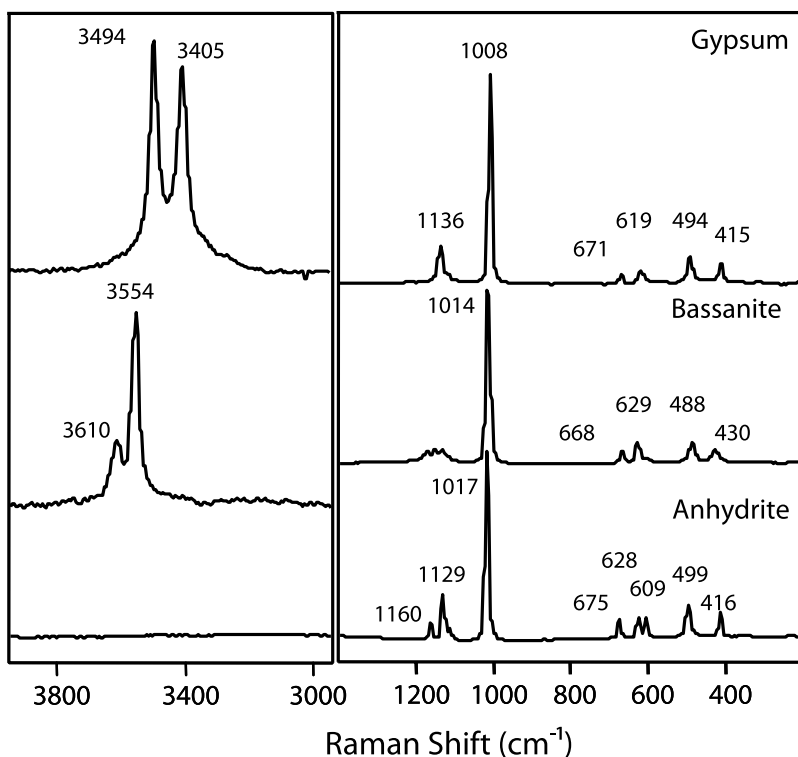


Figure 9. Raman spectra of three Ca-sulfates (anhydrite CaSO_4 , bassanite $\text{CaSO}_4 \cdot 0.5\text{H}_2\text{O}$, and gypsum $\text{CaSO}_4 \cdot 2\text{H}_2\text{O}$). (left) Fundamental vibration modes of structural water and (right) fundamental vibrational modes of $(\text{SO}_4)^{2-}$.

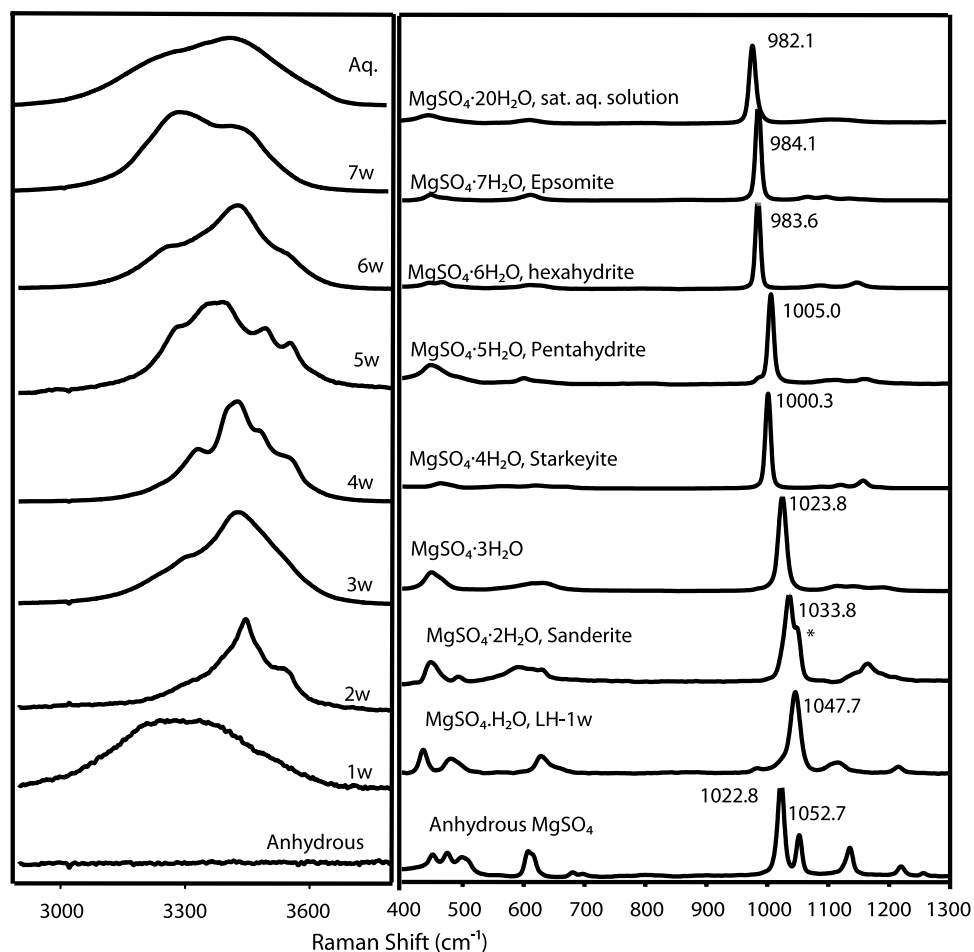


Figure 10. Raman spectra of nine Mg-sulfates (from anhydrous MgSO_4 to aqueous solution). (left) Fundamental vibration modes of structural water and (right) fundamental vibrational modes of $(\text{SO}_4)^{2-}$.

(Tables 2, 3, and 5). These phenomena were also observed by *Chipera and Vaniman [2007]*.

[51] These laboratory experimental observations pose a critical question for the formation mechanism of Martian Mg-sulfate monohydrate, i.e., assuming its precursor was an evaporitic deposit from aqueous solution (i.e., epsomite) as suggested by remote sensing observations [*Mangold et al., 2007*], what was the actual dehydration pathway of epsomite (7w) on Mars? How were the aerielly extensive and thick layers of Martian Mg-sulfate monohydrate formed?

[52] In our experiments, we found that there are two potential pathways to form Mg-sulfate monohydrate from the dehydration of epsomite (7w) in middle to low T-RH range. These pathways are described below.

3.1.1. First Pathway

[53] This pathway is shown in Tables 2 and 5, and especially Figure 2. At 50°C in LiBr and LiCl buffers (6%–11% RH, Table 2), the starting phase epsomite (7w), first converted to amorphous Mg-sulfate (Am) that coexisted with hexahydrate (6w). When the dehydration continued, the water content of Am continued to decrease (demonstrated by a shift of the Raman peak positions of Am toward high wave numbers, Figure 7), and the 1w, 2w, 4w (Figure 2), and 5w (not shown) Mg-sulfates appeared. Later, the amounts of 1w and 2w continued to increase, accompanied by

continuous dehydration of the Am phase (its Raman peak shifted to 1035 cm^{-1}). Eventually, the entire sample became a mixture of LH_1w and 2w Mg-sulfates (Figure 2). When the starting phase was an amorphous Mg-sulfate (about $\text{MgSO}_4 \cdot 2\text{H}_2\text{O}$), as shown in Table 5, it remained amorphous at $\text{RH} \leq 18\%$ (50°C, 21°C, and 5°C), but converted to 1w plus 2w at 31% RH (50°C).

[54] There are several noteworthy differences in Table 2 (7w dehydration) and Table 5 (Am dehydration):

[55] 1. Am \rightarrow 1w + 2w conversion can occur at much lower RH level (6% RH) when the Am coexists with 6w (Table 2). A higher RH (31% RH) was needed to initiate recrystallization from a pure Am phase (Table 5). Either a crystalline phase 6w played a catalytic role in the recrystallization process of Am, or it provided a microscale local environment of higher RH than that of the buffer solution.

[56] 2. Am \rightarrow 1w + 2w conversion occurred at 50°C only, in two systems (from 7w and from Am phase). An intermediate temperature (e.g., 50°C in our experiments) may be needed to provide the energy to initiate the conversion or to increase the rate of conversion. At lower temperatures, we expect this conversion to be very slow.

[57] 3. Similarly, we cannot exclude the possibility of continuous but slow conversion of Am Mg-sulfates to 1w in LiBr and LiCl buffers (Table 5, at the three Ts). The results

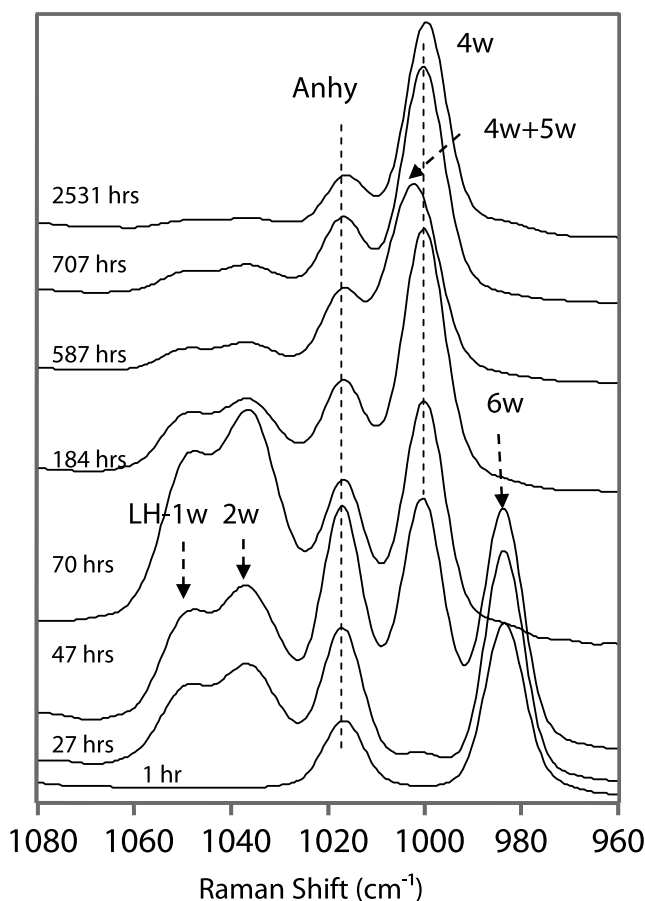


Figure 11. Although the direct dehydration of epsomite in temperature range 50°C to 5°C cannot produce kieserite, monohydrated Mg-sulfate (LH-1w) and sanderite $\text{MgSO}_4 \cdot 2\text{H}_2\text{O}$ were produced at the intermediate stages of dehydration of epsomite $\text{MgSO}_4 \cdot 7\text{H}_2\text{O}$ (at 50°C and 31% RH) when it was originally mixed with anhydrite CaSO_4 .

from continuing experiments at 5°C and -10°C in LiBr, LiCl, and MgCl_2 buffers may provide clarification.

[58] In general, these observations indicate that amorphous Mg-sulfates can be a pathway to form Mg-sulfate monohydrate from evaporitic epsomite (7w) in the middle to low temperature range relevant to current and past Martian surface conditions.

3.1.2. Second Pathway

[59] The second pathway to form Mg-sulfate monohydrate is demonstrated in Figures 11 and 12, by slow dehydration of epsomite (7w) when it is mixed with other phases, for example with anhydrite (CaSO_4). A pure system at 50°C in the MgCl_2 buffer, 6w and 4w are seen at intermediate stages and 4w is the final phase at equilibrium (Table 2). For a starting mixture of epsomite (7w) and anhydrite (Table 6), monohydrate Mg-sulfate (1w), sanderite (2w), hexahydrate (6w), and a trace of starkeyite (4w) appeared during the early stage of dehydration (Figure 11, spectrum at 27 h). The development of 1w + 2w + 4w was accompanied by the continuous reduction of 6w (spectra at 47 h and 70 h). When 6w disappeared, 4w became the major phase, and the percentage of 1w + 2w began to decrease (spectra at 184, 587, and 707 h). Eventually, starkeyite (4w) became the final

Table 7. Molar Compositions of $\text{MgSO}_4 \cdot 7\text{H}_2\text{O}$ Mixed With Ca- and Fe-Sulfates, Fe-Oxides, and Fe-Hydroxides for the Second Set of Mixing Experiments^a

| Phase(s) to be Mixed With Epsomite (mole %) | LiCl Buffer (11.1% RH) | | MgCl ₂ Buffer (30.5% RH) | |
|--|------------------------|--------------------------------------|-------------------------------------|--------------------------------------|
| | Mixed Phase | MgSO ₄ ·7H ₂ O | Mixed Phase | MgSO ₄ ·7H ₂ O |
| FeSO ₄ ·7H ₂ O | 17% | 83% | 17% | 83% |
| CaSO ₄ | 23% | 77% | 25% | 75% |
| Fe ₂ O ₃ | 20% | 80% | 19% | 81% |
| FeOOH | 35% | 65% | 24% | 76% |
| Fe ₂ (SO ₄) ₃ ·7H ₂ O | 8% | 92% | 8% | 92% |
| Fe ₂ (SO ₄) ₃ ·5H ₂ O | 10% | 90% | 9% | 91% |

^aSamples were held at 50°C and in LiCl and MgCl_2 RH buffers.

Mg-sulfate (spectrum at 2531 h) at this set of RH-T conditions. We note that the final product of this experiment (at 50°C and 31% RH) was starkeyite (4w), not 1w and 2w, which suggests that 4w stability was favored over that of 1w and 2w.

[60] During the entire dehydration process (Figure 11), the ν_1 Raman peak of anhydrite was unchanged; that is, no change in its hydration state was observed. A change in the degree of hydration of calcium sulfate would cause a shift of

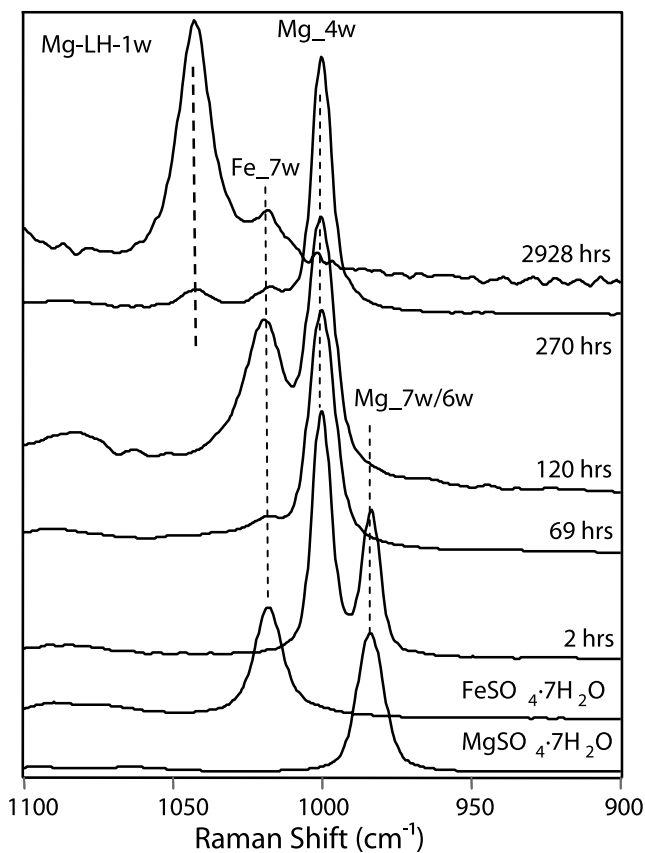


Figure 12. Although the direct dehydration of epsomite at temperature range 50°C to 5°C cannot produce kieserite, monohydrated Mg-sulfate (LH-1w) was produced at the final stage of dehydration of epsomite $\text{MgSO}_4 \cdot 7\text{H}_2\text{O}$ (at 50°C and 11% RH) when it was originally mixed with melanterite $\text{Fe}(\text{SO}_4) \cdot 7\text{H}_2\text{O}$.

Table 8. Gravimetric Measurement Results From Dehydration Experiments at 400°C for MH-1w, LH-1w and Anhydrous Mg-sulfate

| | Grams | Net (g) | Mole |
|---|-------|---------|-----------|
| <i>MH-1w</i> | | | |
| Total mass of empty cup and cover | 22.13 | | |
| Plus MH-1w sample | 23.69 | 1.56 | 1.13E-02 |
| Total mass after baking | 23.47 | -0.22 | |
| Residue (MgSO ₄ by Raman) | | 1.34 | 1.11E-02 |
| Molar mass of MH-1w sample (kieserite 138.37) | | | 140.04 |
| Water per MgSO ₄ in MH-1w | | | 1.09 |
| <i>LH-1w</i> | | | |
| Total mass of empty cup and cover | 21.51 | | |
| Plus LH-1w sample | 23.08 | 1.57 | 1.13E-02 |
| Total mass after baking | 22.84 | -0.24 | |
| Residue (MgSO ₄ by Raman) | | 1.33 | 1.10E-02 |
| Molar mass of LH-1w sample (kieserite 138.37) | | | 141.64 |
| Water per MgSO ₄ in LH-1w | | | 1.18 |
| <i>MgSO₄</i> | | | |
| Total mass of empty cup and cover | 22.98 | | |
| Plus MgSO ₄ sample | 24.58 | 1.60 | 1.33E-02 |
| Total mass after baking | 24.57 | -0.01 | -5.56E-04 |
| Residue (MgSO ₄ by Raman) | | 1.59 | 1.32E-02 |
| Molar mass of the sample (anhydrite 120.37) | | | 120.97 |
| Water per MgSO ₄ in Anhydrous Mg-sulfate | | | 0.01 |

this Raman peak position (Figure 9). In addition, there was no observable cation substitution happening among Mg-sulfate and Ca-sulfates, which would also change their ν_1 Raman peak positions. The peak positions of each sulfate phase that appeared during the reaction (7w, 6w, 4w, 2w, 1w of Mg-sulfates and anhydrite) match with those in the standard spectra (Figures 9 and 10). The samples appeared as solid white powder at all times.

[61] In the second set of mixing experiments, using twelve mixtures of epsomite (7w) with Ca- and Fe-sulfates, Fe-oxide and Fe-hydroxide as starting phases and run at 50°C in LiCl and MgCl₂ buffers (11% and 31% RH), monohydrate Mg-sulfate (1w) was observed in the end products of all systems (e.g., Figure 12). There appeared to be some chemical reactions at intermediate stages during the development of equilibrium in these experiments, which will be a topic of further study.

[62] On the basis of these 18 mixing experiments, we hypothesize that the anhydrous Ca-sulfate, hydrated Fe-sulfates, Fe-hydroxide, and Fe-oxide could have provided a local RH environment surrounding the epsomite (7w) grains. This local RH environment may have overridden the effect of the larger-scale RH environment provided by the humidity buffers and may have facilitated the dehydration of starkeyite (4w) to occur in the middle to low temperature range. In a pure Mg-sulfate system under the same RH-T conditions, the dehydration of starkeyite was inhibited (Tables 2 and 4) owing to the additional activation energy required [Wang et al., 2006c].

[63] We assume that the supply of cations for Martian sulfates was mainly from the weathering of Martian igneous

materials. Fe and Ca cations would be available at the locations where Mg-sulfates precipitated. In a low-intensity weathering of basaltic minerals, i.e., from olivine dissolution as inferred from observations at Gusev Crater by Spirit [Hurowitz et al., 2006], Mg and Fe would be the major cations released. The release of Ca would require either the weathering of pyroxene or feldspar (indicating a higher degree of weathering,) [Nesbitt and Young, 1984; Nesbitt and Wilson, 1992], or the weathering of glassy materials of volcanic origin [Gooding and Keil, 1978]. Glassy materials were identified at Gusev [Ruff et al., 2006; Squyres et al., 2007]. The coexistence of Ca- and Fe-sulfates with Mg-sulfates was inferred by mineral modeling from APXS and Mössbauer data [Clark et al., 2005; Ming et al., 2006; Wang et al., 2006b; Yen et al., 2008] for Meridiani outcrops and Gusev salty soils. Hematite, nanophase Fe-oxides, goethite, jarosite, and ferric sulfates were also identified in rocks and soils at Gusev and Meridiani [Morris et al., 2006a, 2006b, 2008]. These observations support the selection of the minerals used in our mixing experiments.

[64] Nevertheless, sulfates occurring in nature (e.g., Mg-sulfates mixed with Na, K-bearing sulfates, and chlorides as observed in terrestrial saline lake deposits) [Zheng, 1997] are more complicated than we can simulate in a set of laboratory experiments. In general, Mg- and Ca-sulfates do not form a solid solution, but Mg- and Fe-sulfates can form incomplete solid solutions [Jambor et al., 2000]. What would be the dehydration products of (Mg-, Fe-) sulfates if they were the original evaporite phases? More laboratory mixing experiments will be conducted at various RH-T conditions, which will provide further information in the pathways of Martian Mg-sulfate monohydrate formation. The two pathways that we found to form Mg-sulfate monohydrate from evaporitic epsomite (7w) in a middle to low T-RH range indicate that the amorphous Mg-sulfates or coexisting sulfates, oxide, and hydroxide can influence the dehydration process of Mg-sulfates.

3.2. Structural Polymorphs of MgSO₄·H₂O

[65] The formation of Martian Mg-sulfate monohydrate is further complicated by the existence of two structural polymorphs, referred as LH-1w and MH-1w in this paper after their formation conditions (LH stands for low humidity and MH stands for middle humidity). The MH-1w polymorph has a structure identical to the mineral kieserite. These two polymorphs have distinct XRD patterns and Raman and IR spectra as well as distinct formation pathways and stability fields. Both polymorphs can be produced from the same pure reagents MgSO₄·H₂O or MgSO₄·7H₂O.

[66] In order to verify the water content of MH-1w and LH-1w, we did a set of dehydration experiments. Similar masses (1.56–1.6 g) of MH-1w, LH-1w, and anhydrous MgSO₄ were heated to 400°C. The dehydrated products from all three samples were checked by multiple Raman measurements and found to be anhydrous MgSO₄. Gravimetric analysis on these samples (Table 8) confirmed very similar H₂O/MgSO₄ ratios in the original MH-1w and LH-1w samples.

[67] Figure 13 shows the XRD patterns of the two polymorphs. They are also compared with a natural kieserite from Lehrte, Germany [Papike et al., 2008], whose XRD pattern is a perfect match to the standard kieserite in the

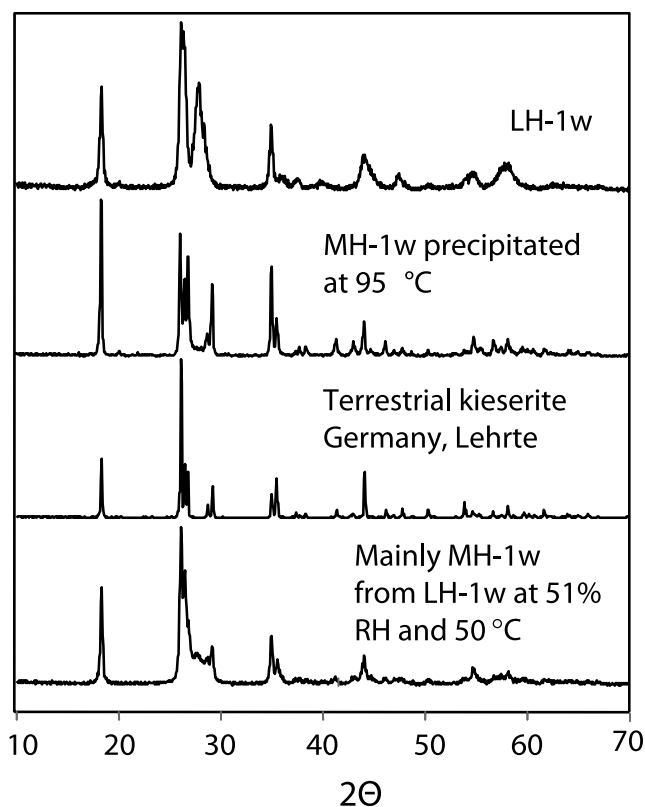


Figure 13. Distinct X-ray diffraction patterns of LH-1w, precipitated MH-1w from aqueous solution at high temperature, natural kieserite, and MH-1w converted from LH-1w at moderate relative humidity.

XRD PDF database and to a calculated XRD pattern based on structural refinement [Hawthorne *et al.*, 1987]. The XRD pattern of MH-1w matches the natural terrestrial mineral kieserite.

[68] Figure 14 shows the Raman spectra of the two polymorphs. They are distinguished by (1) positional differences of the strongest Raman peak, the ν_1 of the SO_4 symmetric stretching vibration mode: 1046 cm^{-1} for LH-1w and 1042 cm^{-1} for MH-1w (kieserite); (2) differences in peak shapes of the OH stretching vibrations in the $3500\text{--}3000\text{ cm}^{-1}$ spectral region due to structural water (singlet for LH-1w and doublet for MH-1w); and (3) differences in positions of other Raman peaks with middle to low intensities. These Raman features are different from those for anhydrous MgSO_4 and all other hydrates of Mg-sulfate from sanderite $\text{MgSO}_4\cdot 2\text{H}_2\text{O}$ to meridianiite $\text{MgSO}_4\cdot 11\text{H}_2\text{O}$ (Figure 10).

[69] Figure 15 shows the mid-IR (ATR) spectra of the two polymorphs. The most obvious difference is that the strongest asymmetric stretching vibration mode ν_3 of the SO_4 tetrahedron is a doublet for LH-1w and a singlet for MH-1w (kieserite). The positions of the ν_1 peak in MIR (weaker and sharper) are consistent with Raman observations (Figure 14). The peak shapes of OH stretching vibrations of the structural water in $3500\text{--}3000\text{ cm}^{-1}$ spectral region (singlet for LH-1w and doublet for MH-1w) are also similar to those in Raman spectra (Figure 14).

[70] In dehydration experiments of the Mg-sulfate monohydrate (Table 4), we found that both structural polymorphs appeared as equilibrium products in the stability field of $\text{MgSO}_4\cdot\text{H}_2\text{O}$ (Figure 4). In more detail, we have the following observations:

[71] 1. LH-1w is the equilibrium phase at $\leq 11\%$ RH at 50°C (2554 h), 21°C (2554 h) and 5°C (17616 h) (in LiBr and LiCl buffers, Figure 4 and Table 4).

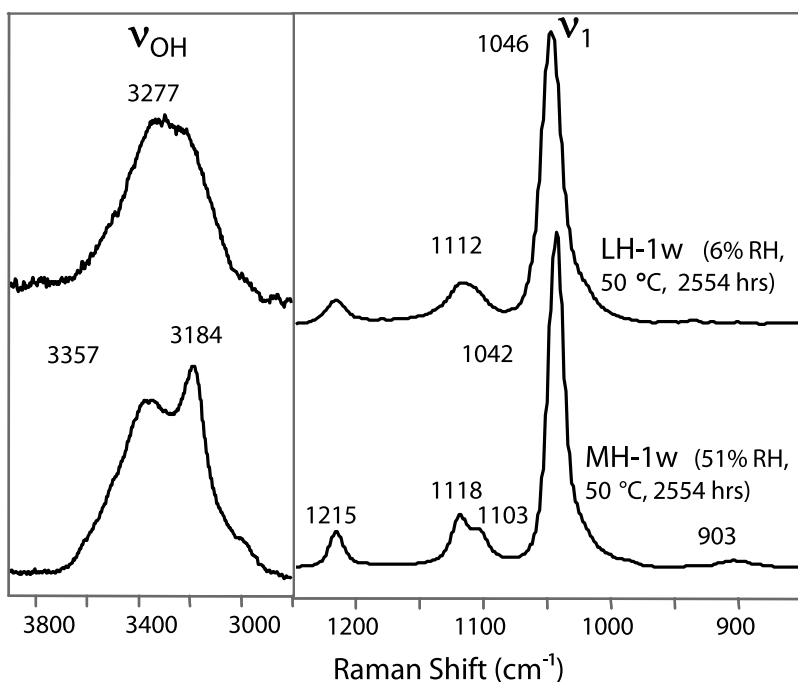


Figure 14. Distinct Raman spectra of LH-1w and MH-1w. (left) Fundamental vibration modes of structural water (ν_{OH}) and (right) fundamental vibrational modes (ν_1 , etc.) of $(\text{SO}_4)^{2-}$.

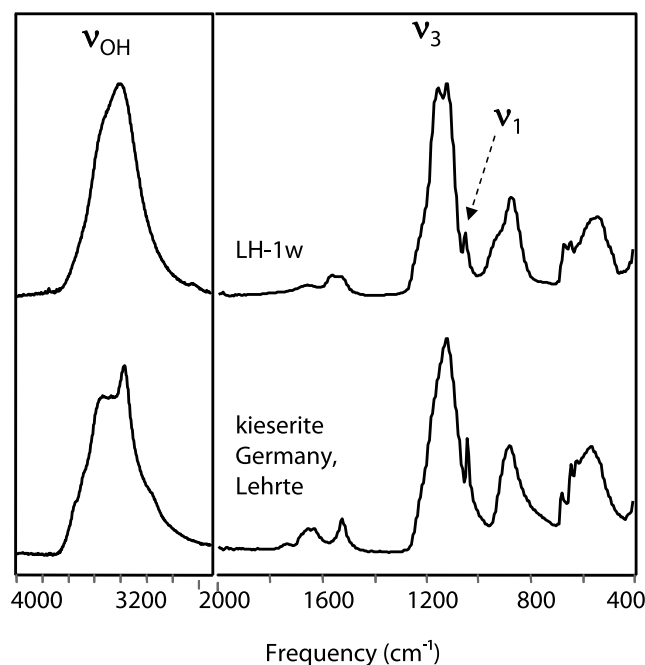


Figure 15. Distinct mid-IR ATR spectra of LH-1w and MH-1w. (left) Fundamental vibration modes of structural water (ν_{OH}) and (right) fundamental vibrational modes (ν_1 and ν_2) of $(\text{SO}_4)^{2-}$.

[72] 2. LH-1w partially converted to MH-1w (kieserite) at 30–54% RH in MgCl_2 and $\text{Mg}(\text{NO}_3)_2$ buffers at 50°C and 21°C (Table 4), appearing as the ν_1 peak position shifted from 1046 cm^{-1} to 1044 cm^{-1} , which is halfway to the 1042 cm^{-1} position of MH-1w ν_1 peak. This suggests that they are mixtures ($1w_{\text{mix}}$) of LH-1w and MH-1w.

[73] 3. LH-1w almost totally converted to MH-1w (kieserite) at 51% RH (in NaBr buffer at 50°C, Table 4 and Figure 14) with ν_1 peak position at 1042 cm^{-1} .

[74] 4. The precipitated polycrystalline phase from a saturated solution of Mg-sulfates at 95°C has a structure of MH-1w (kieserite), with typical XRD (Figure 13) and Raman patterns.

[75] 5. The Mg-sulfate monohydrate, formed through the two dehydration pathways of evaporitic epsomite (7w) discussed in section 3.1, is always LH-1w; that is, it possesses the characteristic Raman spectrum of LH-1w (Figures 8, 11, and 12).

[76] *Chipera and Vaniman* [2007] noticed that a reagent Mg-sulfate monohydrate has a different XRD pattern from the mineral kieserite in the XRD PDF database. In their humidity buffer experiments (using XRD for phase ID of end products), this monohydrate partially converted to kieserite (MH-1w) at middle RH levels (37–53% RH, $T \sim 75$ –23°C), and totally converted to kieserite (MH-1w) at higher RH levels (43–67% RH, $T \sim 75$ –63°C) [*Chipera and Vaniman*, 2007, Table 1]. These observations lead to the following two inferences:

[77] 1. MH-1w (i.e., terrestrial kieserite) only forms at middle to high relative humidity, either directly precipitated from aqueous solution at high temperature (i.e., hydrothermal process, >95°C in our experiments), or slowly converted from LH-1w at middle to high relative humidity and rela-

tively high temperature (i.e., 50°C in our experiments). Some terrestrial natural kieserite (e.g., standard kieserite Lehrte, Germany obtained from the Smithsonian Institution) may have formed in these ways. In our experiments, MH-1w was never observed as the final dehydration product of Mg-sulfates of higher hydration degrees (7w, 6w, or 4w).

[78] 2. On the other hand, LH-1w has been observed as the end phase of the dehydration process of Mg-sulfates of higher degrees of hydration, i.e., from epsomite (7w) and hexahydrate (6w) at high temperature, and from amorphous Mg-sulfate (Am) and mixtures of epsomite (7w) with other minerals at $T \leq 50^\circ\text{C}$. In other words, LH-1w is the ultimate end product of dehydration reactions. We note that under 51% RH and 45% RH at 50°C (Table 4), trace amounts of 6w and 5w appear during the intermediate stage of hydration and MH-1w becomes the dominant phase in the mixtures. This phenomenon indicates that there is a stability field for kieserite (MH-1w) that may partially overlap that of LH-1w. In addition, both polymorphs are stable at low RH. In our dehydration experiments (Table 4), LH-1w was stable at $\leq 11\%$ RH at 5°C, 21°C, and 50°C for 491, 106, and 106 days respectively. In the experiments of *Chipera and Vaniman* [2007], kieserite (MH-1w) was stable at $< 11\%$ RH at 3°C, 23°C, 50°C, 63°C, and 75°C for 117, 97, 70, 91, and 68 days, respectively.

[79] From this set of experimental observations, we hypothesize that most Martian $\text{MgSO}_4 \cdot \text{H}_2\text{O}$ would be LH-1w that originated from dehydration of evaporitic epsomite (7w), hexahydrate (6w), and meridianiite (11w). At locations where hydrothermal processes could raise the local temperatures $> 69^\circ\text{C}$ ($> 342\text{ K}$), MH-1w (i.e., terrestrial kieserite) may occur. We think that the conversion from LH-1w to MH-1w is less likely to happen because that process would require middle to high RH levels to be maintained for a long period of time. Although the large diurnal temperature excursions ($> 100\text{ K}$) at Mars' surface can produce a few hours of high RH in the early morning, the extremely low temperature during early morning hours (-88°C) [*Smith et al.*, 2004] would inhibit the conversion from LH-1w to MH-1w.

[80] Figure 16 shows a scheme for the pathways of forming monohydrated Mg-sulfates (LH-1w and MH-1w) in low-latitude regions on Mars. Epsomite (7w) precipitates directly from Mg-S-enriched aqueous solution when $T < 300\text{ K}$. MH-1w (terrestrial kieserite) precipitates under specific circumstances (hydrothermal processes), when $T > 342\text{ K}$. When relative humidity drops, epsomite, in the absence of other minerals, would undergo partial dehydration that would stop at the stage of starkeyite (4w, by slow dehydration) or amorphous Mg-sulfates (by fast dehydration) as end products. If there were Ca-sulfates, Fe-sulfates, and other minerals coexisting with epsomite, e.g., they were coprecipitated together from Mg, Fe, Ca, S-enriched brine, then epsomite would undergo a more complete dehydration and would end up as LH-1w. Therefore, kieserite (MH-1w), LH-1w, starkeyite (4w), and amorphous Mg-sulfates (Am) would be the end products from dehydration of epsomite of various sources or directly precipitated from Mg-S-enriched hydrothermal fluid. Our experiments show the stability of these minerals within a RH-T range relevant to the current surface and subsurface conditions in low-latitude regions on

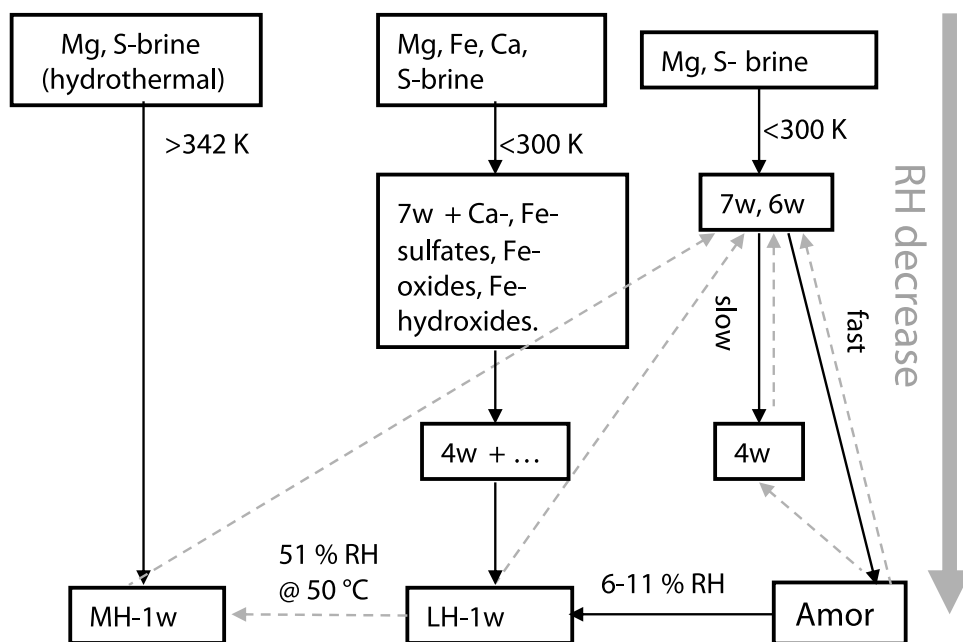


Figure 16. Pathways of forming Martian monohydrated Mg-sulfates (LH-1w and MH-1w) based on the experimental results reported in this paper. Gray dashed lines indicate the potential rehydration pathways of Mg-sulfates in seasonal and diurnal temperature cycles when the relative humidity would be high. However, because of the extremely low temperatures in the period of high RH(s), the rate of rehydration would be very low.

Mars. These minerals should be the most common Martian Mg-sulfate species.

3.3. Stability of Starkeyite (4w)

[81] We postulated in section 2.1 that the stable four-member ring substructural units in starkeyite (4w) may have prevented its further dehydration to form $\text{MgSO}_4 \cdot \text{H}_2\text{O}$ even under extremely low RH at middle to low temperature range ($\leq 50^\circ\text{C}$) (Table 2). If so, then the dehydration process of epsomite (7w) and hexahydrite (6w) in this temperature range would stop at the stage of starkeyite (Figure 1).

[82] Another interesting phenomenon is that starkeyite was the first crystalline phase (or among the first set of crystalline phases) to form during the recrystallization of amorphous Mg-sulfates at all temperatures (50°C , 21°C , and 5°C) and in the full range of relative humidity (6% to 100% RH) in our experiments (Table 5). Furthermore, starkeyite was also the equilibrium product for recrystallization of amorphous Mg-sulfates at several intermediate RH values (Table 5). For example, in Table 5 column 21°C and 33% RH, the phase identified from 1 h to 1309 h shows the progress of recrystallization, which is marked by the appearance of low hydrates (2w, 3w, 4w) first, then the higher hydrates (4w, 5w, 6w). Eventually, starkeyite dominates over other hydrates and is the final equilibrium product. Similarly, starkeyite is the final stable phase during recrystallization of the amorphous phase at 21°C and 39% RH, and at 50°C and 51% RH. Furthermore, during dehydration of a mixture of epsomite and anhydrite at 50°C and 31% RH (Figure 11), starkeyite dominates over 1w and 2w, and becomes the final product within the stability field of $\text{MgSO}_4 \cdot \text{H}_2\text{O}$. We emphasize the distinct difference in these processes from those described earlier, i.e., the direct

dehydration of epsomite that would “stop” at the stage of starkeyite (Table 2). In the two latter processes, starkeyite is the final phase at equilibrium; that is, $\text{MgSO}_4 \cdot \text{H}_2\text{O}$ and $\text{MgSO}_4 \cdot 2\text{H}_2\text{O}$ were rehydrated to form starkeyite. These observations demonstrate that starkeyite has its own stability field in these mid-RH and middle to low T regions, although technically it may be a metastability field [Chou and Seal, 2007].

[83] A comparison of Table 4 (hydration of $\text{MgSO}_4 \cdot \text{H}_2\text{O}$) with Tables 3 and 5 suggests an overlap between the stability field of $\text{MgSO}_4 \cdot \text{H}_2\text{O}$ and the stability field of starkeyite (and that of amorphous Mg-sulfates, Figure 17). Because of the sluggishness of the dehydration process, we have no firm evidence on the extent of this overlap in RH-T space through this set of 138 experiments. Starkeyite keeps its four structural waters under the driest condition for more than 18629 h (Table 3).

[84] To summarize, we make the following three observations: (1) starkeyite is stable at low temperature and low humidity (Tables 2 and 3); (2) it appears as the first phase in the recrystallization process of amorphous Mg-sulfates (Table 5); and (3) it appears as the preferred phase when competing with 1w and 2w at middle to low relative humidity (Figure 11). These observations suggest that starkeyite has the potential to exist on Mars (surface and near surface) and thus to be an important host for the current water budget at the Martian surface.

3.4. Amorphous Mg-Sulfates

[85] Amorphous Mg-sulfate cannot be formed from starkeyite (4w) or $\text{MgSO}_4 \cdot \text{H}_2\text{O}$ (1w). It can only be formed from the rapid dehydration of epsomite (7w) and hexahydrite (6w) for structural reasons [Wang et al., 2006c]. In 1w

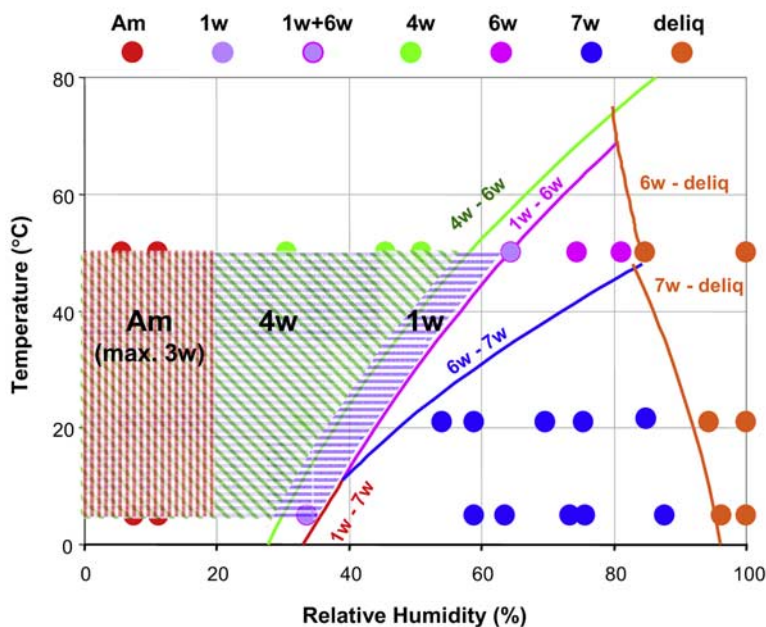


Figure 17. Overview of the stability fields of Mg-sulfates obtained through our experiments. It confirms the phase boundaries and stability fields of epsomite $\text{MgSO}_4 \cdot 7\text{H}_2\text{O}$, hexahydrate $\text{MgSO}_4 \cdot 6\text{H}_2\text{O}$, and their deliquescence relative humidity in a temperature range from 50°C to 5°C . It also confirms the phase boundaries $1\text{w}-6\text{w}$, $1\text{w}-7\text{w}$, and $4\text{w}-6\text{w}$. It demonstrates that the stability (or metastability) fields of monohydrate, starkeyite, and amorphous Mg-sulfates are partially overlapped, and these phases can be stable for long periods of time in the RH-T range that is relevant to Mars. The phase boundary data were kindly provided by I-Ming Chou [Chou and Seal, 2007].

and 4w, the Mg $[\text{O}_x(\text{OH})_{6-x}]$ polyhedra are tightly connected with SO_4 tetrahedra by sharing the bridging oxygen (O_b), thus producing very stable structures. In comparison, the crystal structures of 7w and 6w are loosely packed, evidenced by their large volume per formula unit and their ~ 79 to 88% lower density than 4w. In the hexahydrate (6w) structure, $\text{Mg}(\text{OH})_6$ octahedra and SO_4 tetrahedra are not connected by bridging oxygen, but are instead only weakly linked by hydrogen bonding between the hydrogen atoms of water molecules to the coordinated oxygen of SO_4 . In the epsomite (7w) structure, there is one “free” water molecule that occupies the large spaces among polyhedra but is not coordinated to any of them. The rapid loss of water molecules from 7w and 6w can cause the crystal framework to collapse and to produce amorphous Mg-sulfates (Am). Potentially, amorphization can occur from rapid dehydration of meridianiite ($\text{MgSO}_4 \cdot 11\text{H}_2\text{O}$) that has a polyhedral connection similar to that in 6w and five “free” water molecules.

[86] Vaniman *et al.* [2006] reported the lowest limit on the amount of structural water (water molecules per formula unit, or WMPFU, of MgSO_4) that can be held by amorphous Mg-sulfates as 1.1. From our experiments, we have found the upper limit of the WMPFU for amorphous Mg-sulfates to be about 3. The bold spectra in Figure 18 and the large square symbols in Figure 19a indicate that total amorphization occurred only after a WMPFU value ~ 3 was attained at 21°C and 0°C . These observations are in agreement with experimental results at 50°C during the rehydration process of amorphous Mg-sulfate in eight different relative humidity

buffers, where the Raman and gravimetric measurements indicate the persistence of amorphous structure until a WMPFU value ~ 3.1 was attained (Figure 20). Thereafter, crystalline starkeyite (4w) and epsomite (7w) began to appear from amorphous Mg-sulfate with a WMPFU value > 3.3 . Figure 20 also indicates the ν_1 peak position of amorphous Mg-sulfates shifts monotonically to lower wave number when WMPFU increases. An empirical formula for calculating the water content of amorphous Mg-sulfates based on their Raman peak positions was derived from these observations (see Figure 7). Results shown in Figure 19 (21°C , 0°C) and Figure 20 (50°C) suggest that the temperature (in our experimental range) does not have an obvious effect on the highest water content of an amorphous Mg-sulfate. The upper limit of WMPFU of amorphous Mg-sulfates has important implications for the current water budget at the surface and near surface of Mars.

[87] Our experiments also reveal that there are two ways to create Am from 7w and 6w. One way is through rapid dehydration, i.e., by placing the samples into a desiccator under a rough vacuum (up to 60 mtorr) for ~ 2 h at 21°C (Figure 18). The absolute water vapor pressure in the desiccator during these experiments was in the range of annual water vapor pressures at equatorial regions on Mars, e.g., 0.04 – 0.15 Pa [Smith, 2002]. The second way is to form amorphous Mg-sulfates at one atmosphere pressure but at extremely low relative humidity (6% RH in Table 2) and with a moderate dehydration rate (24 to 224 h). In general, the essential condition to form an amorphous structural framework is the capability to remove the water molecules that

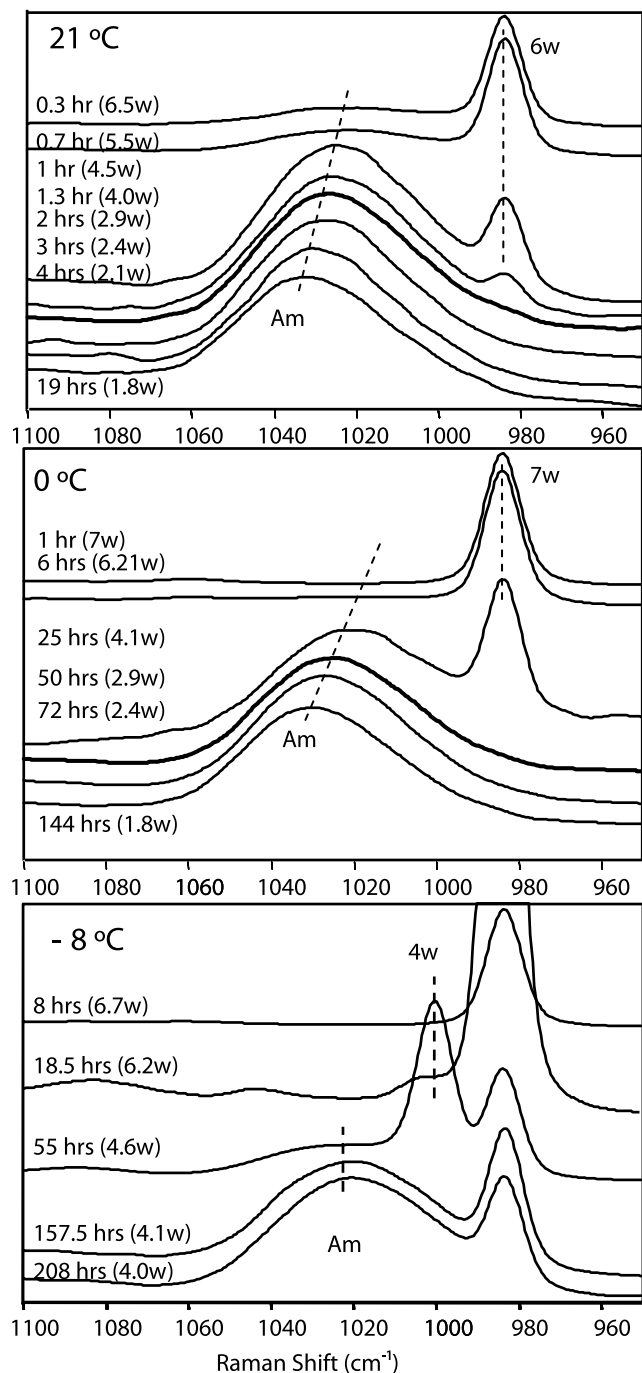


Figure 18. Raman spectra of intermediate and final products from the amorphization of epsomite at 21°C, 0°C, and -8°C. The bold spectrum in each plot marks the total amorphization. The large time difference for reaching the total amorphization at different temperatures (2 h at 50°C and 50 h at 21°C) indicates a significant reduction of reaction rate at low T. The appearance of starkeyite (4w) at -8°C implies that a competition between amorphization and normal dehydration may favor the latter at even lower T. Note the Raman peak position of amorphous Mg-Sulfate shifts toward high wave number (cm^{-1}) when Am dehydration continues.

were originally attached to Mg in octahedral coordination and to collapse the crystalline structure. Temperature does have an obvious effect on the amorphization, as evidenced by the fact that the amorphous phase was only formed by slow dehydration at 50°C, but not by experiments done at 21°C and 5°C at the same RH levels (Table 2). The magnitude of molecular thermal vibrations may drive the destabilization of structural water molecules from epsomite (or hexahydrate). Results shown in Table 5 indicate that the amorphous Mg-sulfates were extremely stable at low T and low RH (17616 h at 5°C, $\leq 11\%$ RH).

[88] The goal of our experiments in studying vacuum dehydration at 21°C, 0°C, and -8°C was to test the temperature effect on the formation of amorphous Mg-sulfates and to quantify the rate of amorphization as a function of temperature. The time to achieve the total amorphization of the same

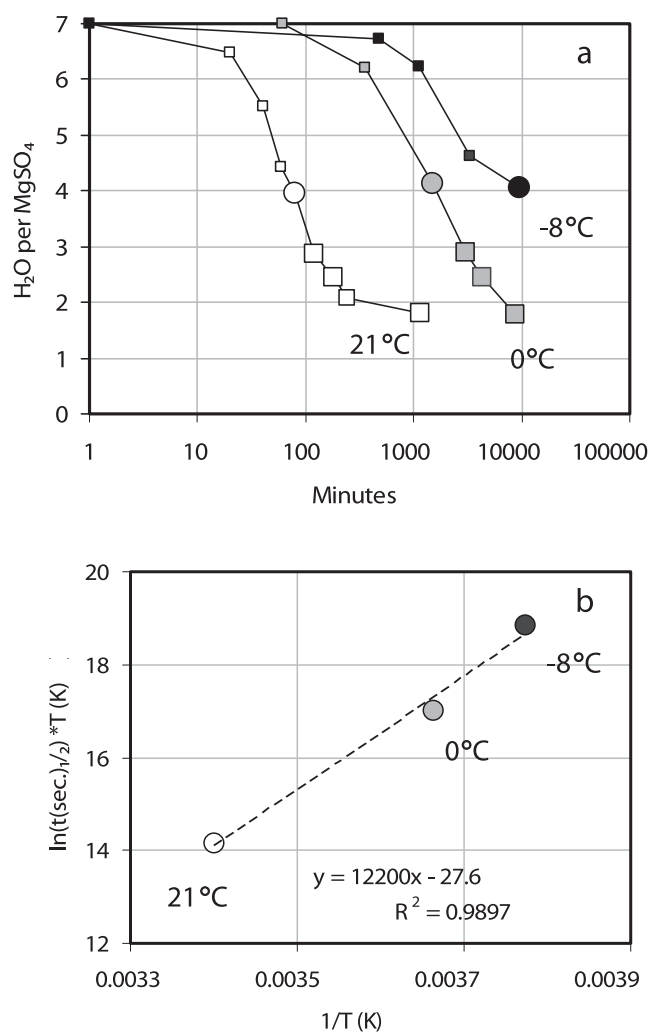


Figure 19. Rates of amorphization from epsomite at three temperatures (21°C, 0°C, and -8°C). Because of limited number of experimental data (and the difficulty in conducting low T vacuum experiments), we are not certain if the regression line in Figure 19b should actually be a straight line. The dehydration mechanism at low T can change, such as the competition between amorphization and normal dehydration suggested by the appearance of starkeyite at -8°C (Figure 18).

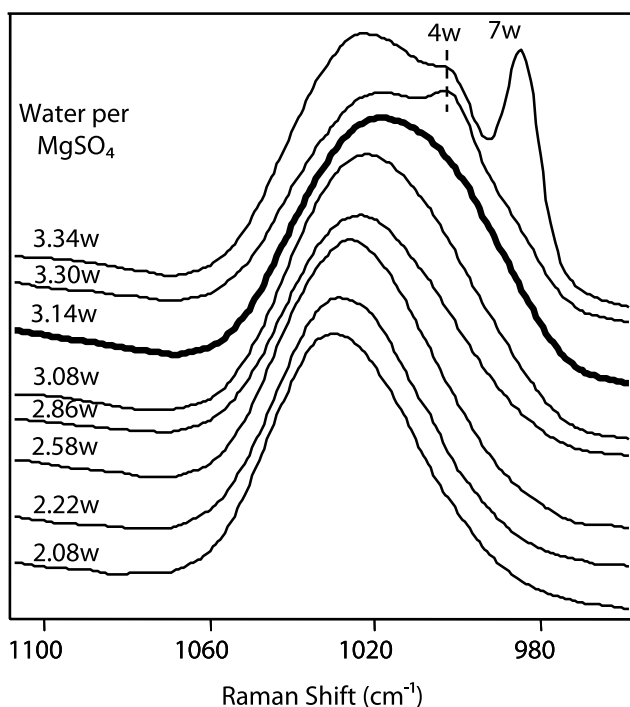


Figure 20. Raman spectra obtained during the rehydration process of amorphous Mg-sulfates. The bold spectrum marks the highest WMPFU held by an amorphous Mg-sulfate (3.14w). Crystalline starkeyite ($\text{MgSO}_4 \cdot 4\text{H}_2\text{O}$) started to appear in Am sample when WMPFU further increases (3.3w).

mass of sample increases greatly as temperature drops (Figure 18). Raman spectra in Figure 18 show that at 21°C , ~ 50 mg epsomite (7w) totally converted to amorphous Mg-sulfate in 2 h (bold spectrum). The same mass of epsomite took 50 h to achieve a total amorphization at 0°C (bold spectrum). At -8°C , total amorphization was not reached even after 208 h.

[89] Figure 19 shows the results of gravimetric measurements on three sets of vacuum dehydration experiments. Although the absolute rate of amorphization would relate to specific experimental setting, the relative amorphization rates appear to be inversely correlated with the experimental temperature. Since epsomite (7w) can readily lose one water molecule to become hexahydrate (6w), the conversion from hexahydrate (i.e., WMPFU = 6) to amorphous Mg-sulfate (WMPFU ~ 2 in our experiments) would be the rate-limiting step during the amorphization process. We can use the time needed to reach a WMPFU value ~ 4 as the approximate half-life ($t_{1/2}$) of the process, which is represented by the three large circular symbols in Figure 19a. A combination of the first-order rate equation with the Arrhenius equation shows that the temperature dependence of $t_{1/2}$ can be expressed by

$$\ln[t_{1/2} * T] = [G^* / R][1/T] - \ln[0.693k_B/h]$$

where R , k_B and h are the universal gas constant, Boltzmann's constant, and Planck's constant, respectively, and G^* is the activation free energy for the process. By

putting our experimental data into a $\ln[t_{1/2} * T]$ versus $(1/T)$ plot (Figure 19b), it appears that a linear regression line can fit the experimental data with a $R \approx 0.990$ ($R = 0.988$ is significant at the 90% level for three points). This fit suggests that the amorphization process matches a first-order forward reaction whose rate can be estimated by $k(T) = \ln 2/t_{1/2}(T)$. Thus the reaction rate k at 21°C is 18.6 times the k at 0°C , and 118 times the k at -8°C .

[90] This set of observations suggests that in the temperature range at the present-day Martian surface, the time required for total amorphization of epsomite powder could be very long. The observed surface temperature range at Meridiani by MER [Smith *et al.*, 2004, 2006] is about 285–180 K in the aphelion season, and slightly warmer (~ 10 K) in the perihelion season. During a diurnal cycle, the most rapid RH decrease (from 100% to 0% due to rapid temperature decrease) would occur in the early morning. That rapid RH decrease could induce rapid dehydration, i.e., the amorphization of Mg-sulfates. Nevertheless, the temperature during that period would be in the range of 180–220 K. By extrapolating the regression line in Figure 19b to this temperature range, we find that over a hundred to as high as 20 million Earth years would be needed for epsomite to reach a WMPFU ≈ 4 . As we stated, a critical condition to form amorphous Mg-sulfates is to rapidly extract water molecules from epsomite or hexahydrate that will cause structural collapse. This condition may not be satisfied if the reaction rate is too slow.

[91] During experiments at -8°C , a Raman peak at 1000 cm^{-1} belonging to the ν_1 mode of starkeyite (4w) was observed in the intermediate dehydration products taken out of vacuum at 18.5 h and 55 h (Figure 18, -8°C), where evidence of amorphous Mg-sulfate was also found (55 h Figure 18, -8°C). The peak of starkeyite was not observed in the later dehydration products (157.5 and 208 h in Figure 18, -8°C), where a large amount of amorphous Mg-sulfate was found. Competition between the formation of starkeyite and the formation of the amorphous phase seems to have occurred. In low-T vacuum dehydration experiments where the dehydration rate was reduced by several orders of magnitude, the appearance of starkeyite is not unexpected because starkeyite is the common end product of slow dehydration from epsomite (Table 2).

[92] In a temperature range much lower than -8°C , e.g., the early morning hours at the current surface of Mars (approximately -88°C) [Smith *et al.*, 2004], where the rate of dehydration would decrease further, the possibility of starkeyite (4w) as the end product of dehydration of epsomite, instead of amorphous Mg-sulfate, would increase greatly. In that sense, amorphous Mg-sulfate may not be formed as readily as anticipated by Vaniman *et al.* [2004] during the diurnal cycle at the Martian surface. In addition, because of the stable four-member rings in the starkeyite structure, starkeyite converts less readily than the amorphous phase to higher hydrates (Tables 3 and 5). The combination of these two possibilities would lead a lower abundance of amorphous Mg-sulfates than starkeyite.

3.5. Longevity of Hexahydrate (6w) at Low RH

[93] We have found that the dehydration of hexahydrate (6w) is a process depending on many factors. Temperature is obviously a major factor. For example, at 50°C with RH \leq

31% hexahydrite (6w) converted entirely to starkeyite (4w) after 24 h in our experiments (Table 2), whereas at 5°C and lower RH (7% and 11%), a trace of 6w still remained after 12802 h (Table 2).

[94] On the other hand, the coexistence of other mineral phases appears to have a significant effect on the dehydration rate of hexahydrite. In comparison with a total conversion of pure 6w to 4w after 24 h of dehydration (RH \leq 11% at 50°C, Table 2), detectable traces of 6w remained after 686 h at a lower RH (6% RH and 50°C) in a mixture with amorphous Mg-sulfates (Table 2). When 6w was initially mixed with Ca-sulfates, 6w persisted in the dehydration products as a trace component even after 2531 h when mixed with anhydrite, 248 h when mixed with gypsum, and 69 h when mixed with bassanite (Table 6). We suspect that the local-scale RH environment made by coexisting phases could be responsible for the decrease of the dehydration rate of 6w. Reduction of the dehydration rate of 6w by low temperature and coexisting mineral phases would have important implications for the hydration states of Martian Mg-sulfates and for the current water budget on Mars.

4. Applications of Experimental Results

4.1. Comparison With Orbital Remote Sensing Spectra From Mars

[95] Because of large seasonal and diurnal temperature cycles on Mars and the low reaction rates for dehydration, rehydration, amorphization, and recrystallization of Mg-sulfates at low temperature demonstrated in this study, equilibria in these processes may not be reached on the Martian surface. As a result, the phases that would appear at intermediate stages, i.e., starkeyite (4w), amorphous Mg-sulfates (max \sim 3w), to some extent hexahydrite (6w), and their persistence at low RH would have very important implications for the hydration states of current Martian sulfates and water budget on Mars. On the basis of experimental observations, we suggest that Mg-sulfates with intermediate to high degrees of hydration do have the potential to be present on Mars today, especially in the equatorial regions where high levels of hydrogen have been detected by the neutron spectrometer (NS) on Mars Odyssey [Feldman *et al.*, 2004].

[96] The NS results indicate 6–7 wt % water-equivalent-hydrogen (WEH) within the subsurface regolith (<1 m) in the vicinity of Gusev Crater [Feldman *et al.*, 2004], where, among other things, the Mars Exploration Rover Spirit has excavated light-toned, salty soils at various locations. The analysis of seven Pancam multispectral observations obtained from a salty soil at a target site called “Tyrone” over 198 sols suggests that dehydration might have occurred in the salty soils after its exposure to the current Mars surface environment [Wang *et al.*, 2008a]. This observation suggests an RH gradient in the subsurface regolith of that site; that is, RH at depth was less affected by the Martian atmosphere and was instead buffered by hydrated salts buried at that level and deeper. A RH gradient and high(er) RH in subsurface regolith would help to maintain the stability of Mg-sulfates of intermediate to high degrees of hydration such as starkeyite (4w), an amorphous phase (1.1w–3w), and hexahydrite (6w).

[97] Comparing a spectrum of polyhydrated sulfates obtained by the OMEGA instrument on Mars Express with the NIR reflectance spectra of Mg-sulfates of intermediate to high hydration states (4w, Am, 6w, and 6w + Am, Figure 21), it appears that the absorption bands near 1.9 μm of starkeyite (4w) and amorphous Mg-sulfates (containing 1.8w to 2.9w, WMPFU) have a very similar band shape and the approximate central wavelength to the corresponding band of the polyhydrated sulfates. Unfortunately, the low S/N ratios of OMEGA spectra prevent further extraction of spectral details. These two phases (4w and Am) also have a spectral plateau that starts near 2.4 μm , with similar relative band depth(s) and similar shoulder wavelength(s) as the similar plateau of the OMEGA polyhydrated sulfates spectrum. The degree of hydration of the amorphous Mg-sulfate (from 1.8w to 2.9w) does not affect the general spectral shape, the central wavelength of the absorption band near 1.9 μm spectral band, and the “shoulder” wavelength of the spectral plateau near 2.4 μm . It does affect the width of band near 1.9 μm and the slope between 1.9 to 2.3 μm . Therefore, the spectral similarity suggests that both starkeyite and amorphous Mg-sulfates are good candidates for the sites where the polyhydrated sulfates were assigned on the basis of OMEGA spectra. For hexahydrite (6w) and the mixtures of hexahydrite with amorphous Mg-sulfates (6w + Am), their central wavelength of the band near 1.9 μm seems slightly longer than that of OMEGA polyhydrated sulfates (Figure 21, shifts caused by the addition of 6w); thus, these are less likely to be candidates, but they cannot be totally excluded because of the low S/N ratios of OMEGA spectra.

[98] Kieserite or Mg-sulfate monohydrate was identified by OMEGA (Mars Express) [Arvidson *et al.*, 2005] and by CRISM (MRO) [Murchie *et al.*, 2007b] on the basis of three major spectral features (Figure 22), an absorption band centered at 1.95 μm , a wide absorption with a maximum near 2.06 μm , and a weak absorption started near 2.39 μm . A comparison with the spectra of Mg-sulfate monohydrates, MH-1w, LH-1w, and Fe²⁺-sulfate monohydrate, precludes the last one as a candidate owing to the differences in its central wavelength(s) of 1.99, 2.09, and 2.40 μm . The two polymorphs of Mg-sulfate monohydrates, MH-1w and LH-1w, have distinct band positions and band shapes in NIR reflectance spectra (Figure 22), but the differences are less prominent compared with those in Raman and mid-IR spectra (Figures 14 and 15). The positions of the absorption bands for LH-1w are 1.95, \sim 2.06, and 2.38 μm , for MH-1w (kieserite) are 1.97, \sim 2.06, and 2.39 μm . In addition, the 2.06 μm band of MH-1w has a flattened top that may relate to its double peaks in the water fundamental vibration region (Figures 14 and 15). In general, the spectral features of LH-1w show a better match to the typical OMEGA spectrum of Martian monohydrated Mg-sulfates (Figure 22). This suggests that the most observed monohydrated Mg-sulfates on Mars are possibly the dehydration products from Mg-sulfates with higher hydration states (7w, 6w, 11w) that were precipitated in the past from aqueous solutions.

[99] The laboratory study on the formation pathways and stability fields of two structural polymorphs of MgSO₄·H₂O (MH-1w and LH-1w) provides important clues to the origin of Martian Mg-sulfate monohydrates. If a MH-1w (terrestrial kieserite) spectrum were to be found at a particular location on Mars, it might signify the presence of a past hydrothermal

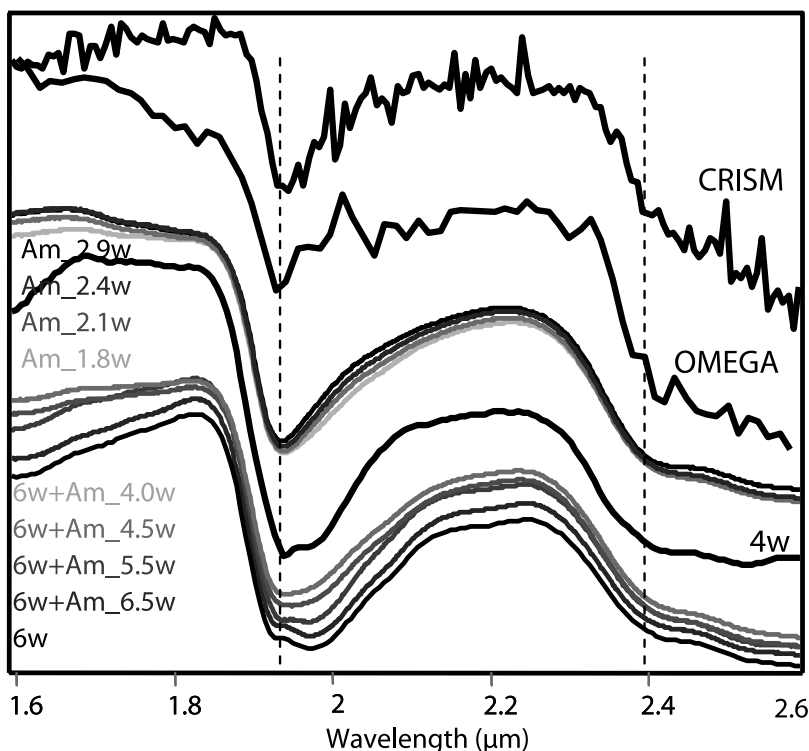


Figure 21. Laboratory NIR reflectance spectra of amorphous Mg-sulfates (with different WMPFU), starkeyite $\text{MgSO}_4 \cdot 4\text{H}_2\text{O}$, and the mixtures of hexahydrate (6w) and Am (different mixing ratios) have a similar spectral pattern but are different in band widths and in band shapes. They are compared with the typical spectral pattern of polyhydrated sulfate obtained by OMEGA and CRISM instruments.

system, which is of special interest as a favorable environment for bio-organism habitability. Nevertheless, because of the minor differences in spectral features of MH-1w and LH-1w in the NIR region, further study to improve the S/N of OMEGA and CRISM spectra will be needed to confidently distinguish these two polymorphs on Mars.

4.2. Contribution From Mg-Sulfates to Water Budget on Mars

[100] Candidates to explain the enhanced hydrogen detected by the Odyssey neutron spectrometer include hydrated minerals and ground ice. Whether ground ice would be stable in the uppermost meter at equatorial latitudes depends on the local thermal gradient, which is a function of the thermal conductivities of underlying materials, the porosity of the regolith, and the concentration of water in various phases [Mellon *et al.*, 2004].

[101] Among hydrated minerals, phyllosilicates, zeolites, and salts (mainly sulfates) are the major candidates that have been considered [Clark *et al.*, 1976, 1982; Clark, 1993; Ruff, 2004; Bish *et al.*, 2003, Vaniman *et al.*, 2004; Chou and Seal, 2007; Wang *et al.*, 2006c, 2008b]. However, in order to match the WEH level detected by the NS in the vicinity of Gusev, large concentrations of phyllosilicates would be needed. Even in their pure forms (without mixing with basaltic components), only a few phyllosilicates can hold >6 wt % water in their structures [Deer *et al.*, 1966]. Common phyllosilicates in the smectite group (e.g., montmorillonite, saponite, and nontronite) can contain >10 wt % water depending on the type of interlayer cations [Bish *et al.*, 2003; Chipera *et al.*, 1997]. Minerals in the kaolinite-

serpentine group (e.g., nacrite, dickite, and halloysite) can maintain up to 14 wt % water.

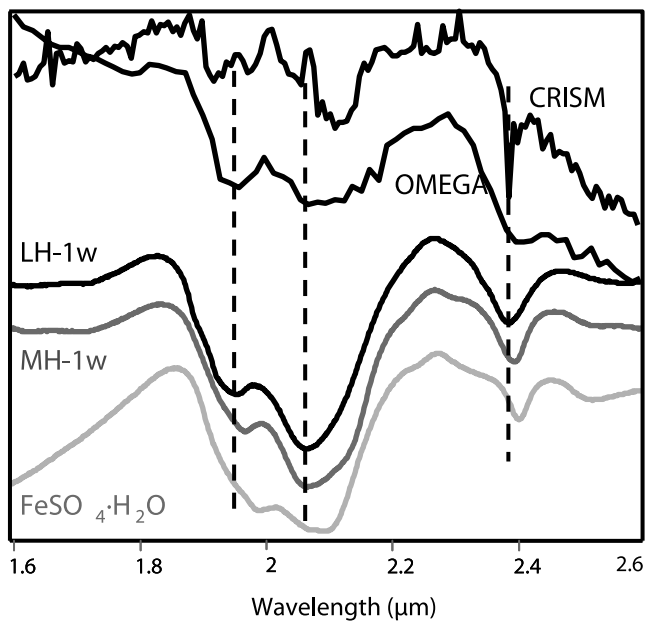


Figure 22. Laboratory reflectance NIR spectra of LH-1w, MH-1w, and $\text{FeSO}_4 \cdot \text{H}_2\text{O}$ have different band centers and band shapes. They are compared with the typical spectral pattern of kieserite obtained by OMEGA and CRISM instruments.

[102] The water storage capabilities of some sulfates can be extremely high compared to phyllosilicates [Deer *et al.*, 1966]. Hydrated Mg-sulfates, with nine unique hydration states (from one to eleven structural waters per $(\text{SO}_4)^{2-}$ plus hydrated amorphous phases) can hold 13–62 wt % structural water. The full-scale swing in relative humidity (from almost 0% to 100% RH) during a Martian diurnal cycle [Smith *et al.*, 2004, 2006] can induce a series of changes in the hydration states of Mg-sulfates at the Martian surface, as demonstrated in this and other studies. The two hydration states of Ca-sulfates hold less structural water (6.2–20.9 wt %), and the vapor-solid transitions between them are relatively slow [Hardie, 1967; Blount and Dickson, 1973; Møller, 1988]. Ferric sulfates may be more important than Ca-sulfates for the current water budget at equatorial latitudes on Mars because they can hold 20–50 wt % water in their structures [Deer *et al.*, 1966]. Fe^{3+} -bearing sulfates were indeed detected by Mössbauer spectral analysis in the Meridiani outcrop and also in the salty soils at Gusev [Morris *et al.*, 2006a, 2006b, 2008].

[103] For example, Spirit has revealed over ten occurrences of salty soils in the part of Gusev Crater where it has been active [Wang *et al.*, 2008a]. If we take the degree of hydration of the sulfates identified by OMEGA, MER, and CRISM, i.e., $\text{MgSO}_4 \cdot \text{H}_2\text{O}$ for Mg-sulfates, jarosite for Fe-sulfates, and gypsum for Ca-sulfates, to calculate the total water contents in these salty soils, it would be too low to match the 6–7 wt % WEH in the regolith of the broad area (~ 600 km foot print) suggested by the neutron spectrometer results. However, when considering the potential existence on Mars of the sulfates with intermediate to high hydration states as suggested by our experimental results, i.e., taking starkeyite ($\text{H}_2\text{O}/\text{SO}_4 = 4$) for the Mg-sulfates and copiapite ($\text{H}_2\text{O}/\text{SO}_4 = 3.3$) for ferric sulfates [Ling *et al.*, 2008a], the maximum water content of some salty soils at Gusev could be as high as 25 wt %. Similarly, the total water content of the Meridiani outcrop could be as high as 13 wt % [Wang *et al.*, 2008a, Table 4]. These calculations indicate that laboratory experimental studies on the stability field of Mg-sulfates with midlevel hydration can help link the surface exploration results to orbital remote sensing data and address questions about the current water budget on Mars and its hydrological history.

5. Conclusions

[104] This study of the stability relationships and phase transition pathways of Mg-sulfates provides a comprehensive view about how the Mg-sulfate species at equilibrium or during the development of equilibrium of hydration/dehydration processes are affected by temperature, relative humidity, starting phases, and coexisting phases. In a temperature range relevant to current and past Martian surface conditions, there are two most likely pathways to form Mg-sulfate monohydrates from the dehydration of epsomite or hexahydrate.

[105] Our experiments indicate that starkeyite (4w) and amorphous Mg-sulfates (max 3w) can (1) appear frequently at intermediate stages of dehydration and rehydration processes of Mg-sulfates, (2) persist in a middle to low temperature range (5–50°C) and extremely low relative humidity

($\sim 6\%$ RH), and (3) have NIR spectral patterns similar to those of polyhydrated sulfates; thus, they are good candidates for the site where polyhydrated sulfates have been indicated by OMEGA and CRISM spectra. The existence of Mg-sulfates with intermediate degrees of hydration at the MER sites would help to explain the high WEH levels found by the neutron spectrometer on Mars Odyssey. Furthermore, because of the strong temperature dependence of the amorphization rate, we anticipate a competition between the formation of amorphous Mg-sulfates and the formation of starkeyite during the diurnal temperature cycle at the surface of Mars. Lower temperature would favor the latter process, and would lead a lower abundance of amorphous species than of starkeyite.

[106] Two structural polymorphs of Mg-sulfate monohydrate were discovered during this study and were characterized using various spectroscopic methods. Because these two polymorphs have different formation pathways, to distinguish them during the current and future missions to Mars can provide important information on geological processes such as the occurrence of hydrothermal activity.

[107] Martian sulfates may have been deposited billions of years ago [Bibring *et al.*, 2006a, 2006b]; however, changes in environmental conditions have likely caused various phase transitions and alteration since the time of original deposition. Laboratory simulation experiments can provide important insight to understand these processes at the surface and subsurface on Mars.

[108] At the time of writing, we are continuing 12 experiments with four starting Mg-sulfates at 5°C within LiBr, LiI, and MgCl_2 buffers, and 30 experiments with five starting Mg-sulfates at -10°C using six humidity buffers. The results of these experiments should provide further information on the stability of these Mg-sulfates at lower temperature and on the exact location of the 11w–7w phase boundary in a relevant RH-T range.

Appendix A: Samples and Experiments

A1. Mg-Sulfate, Ca-Sulfate, Fe-Sulfate, Fe-Oxide, and Fe-Hydroxide Samples

[109] Two chemicals were used to prepare all four hydrated Mg-sulfates as starting phases in our experiments. They are monohydrated $\text{MgSO}_4 \cdot \text{H}_2\text{O}$ (1w, Sigma-Aldrich 434183, Batch 12426BC) and septahydrate $\text{MgSO}_4 \cdot 7\text{H}_2\text{O}$ (7w, Sigma Aldrich M5921, batch 084k0106). Samples were hand ground and sieved to $<75 \mu\text{m}$ grain size to ensure sufficient surface area to interact with water vapor. We chose to do our experiments on one grain-size range because Vaniman and Chipera [2006] demonstrated that notable grain-size effects only occur in the first 2–10 h of hydration and dehydration processes. Beyond that time period, all size fractions follow the same gravimetric variations at a given temperature. In addition, special attention was paid to prepare the four starting phases in pure hydration states to ensure meaningful gravimetric measurements. For example, in order to have a pure monohydrate Mg-sulfate sample as starting phase, $\text{MgSO}_4 \cdot \text{H}_2\text{O}$ powder was baked at 90°C to remove minor amounts of hexahydrate. For epsomite sample, $\text{MgSO}_4 \cdot 7\text{H}_2\text{O}$ powder was equilibrated at 75% RH at 21°C to remove minor amounts of hexahydrate (6w, $\text{MgSO}_4 \cdot 6\text{H}_2\text{O}$). This was done

by storing the sample in a sealed desiccator that contained a saturated aqueous solution of NaCl. Amorphous Mg-sulfate (Am, $\text{MgSO}_4 \cdot 2\text{H}_2\text{O}$) was made from $\text{MgSO}_4 \cdot 7\text{H}_2\text{O}$ powder ($<75 \mu\text{m}$) by rapid vacuum desiccation at no more than 0.8 Pa water vapor pressure at room temperature. Starkeyite (4w, $\text{MgSO}_4 \cdot 4\text{H}_2\text{O}$) was made from $\text{MgSO}_4 \cdot 7\text{H}_2\text{O}$ powder ($<75 \mu\text{m}$) by dehydrating the 7w at 30% RH at 50°C in a sealed desiccator containing a saturated aqueous solution of MgCl_2 . The structures of four starting phases were confirmed by XRD measurements. Multipoint (>20 sample points) Raman microprobe measurements were made on each of these materials to ensure their homogeneity.

[110] Three Ca-sulfates were used for powder mixing experiments with epsomite: anhydrite (CaSO_4 , Sigma-Aldrich 237132 batch 13614Pb), bassanite ($\text{CaSO}_4 \cdot 0.5\text{H}_2\text{O}$, Fisher Chemicals 30766 batch 15228BA), and gypsum ($\text{CaSO}_4 \cdot 2\text{H}_2\text{O}$, Fisher Chemicals, 87676). No additional sample preparation was used for the Ca-sulfates because under normal laboratory conditions their hydration/dehydration reactions are extremely slow [Hardie, 1967; Blount and Dickson, 1973; Møller, 1988]. Among the three Fe-sulfates used in the powder mixing experiments, $\text{FeSO}_4 \cdot 7\text{H}_2\text{O}$, $\text{Fe}_2(\text{SO}_4)_3 \cdot 7\text{H}_2\text{O}$, and $\text{Fe}_2(\text{SO}_4)_3 \cdot 5\text{H}_2\text{O}$, the first one was purchased from ACROS (201390010. Lot A0242021) and the latter two were synthesized in our laboratory [Ling *et al.*, 2008a, 2008b]. The hematite (Fe_2O_3) and goethite (FeOOH) samples used in powder mixing experiments are synthesized samples, kindly provided by R. V. Morris of Johnson Space Center. The purity and homogeneity of samples described in this paragraph were confirmed by multipoint Raman microprobe measurements.

A2. Hydration/Dehydration Experiments

[111] A humidity buffer technique was used to create environments with stable RH at constant temperatures [Greenspan, 1977; Chou *et al.*, 2002]. Depending on the selected experiment temperature, the samples were exposed to fixed RH's over a period of several hundred to over 10,000 h in order to simulate long-term static dehydration/hydration processes on Mars. Twelve humidity buffers based on saturated aqueous solutions of binary salts were used giving a range of RH's from 6% to 100% (Table 1). The relative humidity maintained by these saturated solutions changes with temperature. Thirty experiments were conducted for each of the four starting Mg-sulfates with ten humidity buffers to cover the full range of relative humidity at each of three temperatures, $21 \pm 1^\circ\text{C}$ at laboratory ambient, $5 \pm 1^\circ\text{C}$ in a refrigerator, and $50 \pm 1^\circ\text{C}$ in an oven. Using a humidity/temperature/dew point meter, we found that the RH uncertainty in our RH buffers was $\pm 1\%$.

[112] A thin layer of starting Mg-sulfate powder (~ 0.2 g in most cases, ~ 0.1 g for LiI and NaI buffers, all within a grain-size range $<75 \mu\text{m}$) were placed in straight wall Kimax[®] scintillation vials of 25 mm diameter (20 ml). These reaction vials were placed in 60 mm diameter (4 oz) straight wall glass jars containing the humidity buffer solutions. The reaction vials used for powder mixing experiments were 12 mm in diameter, and were placed into straight wall Kimax[®] scintillation vials of 25 mm diameter containing the humidity buffer solutions. The humidity

buffer jars/vials were tightly capped and stored in lab ovens, or refrigerators held at fixed temperature for the duration of the experiment.

A3. Special Experiments for Amorphous Mg-Sulfates

[113] Amorphous Mg-sulfate (Am) has been proposed to be one of the major forms of Mg-sulfate present over broad regions of Mars [Vaniman *et al.*, 2004]. We have previously reported the formation, within 2 h, of amorphous Mg-sulfate by rapid vacuum dehydration of epsomite placed in a vacuum desiccator at room temperature ($21 \pm 1^\circ\text{C}$). Addition vacuum dehydration experiments were done where the temperature of the desiccator was maintained at either $0 \pm 0.5^\circ\text{C}$ using a water-ice bath, or at $-8 \pm 3^\circ\text{C}$ using a KCl – water ice bath. A 60 millitorr vacuum was attained in the desiccator. With a RH range of 22–36% in our laboratory, the approximate water vapor pressures inside the vacuum desiccator during the period of these experiments was estimated to be within the range of annual water vapor pressures at equatorial regions on Mars, e.g., 0.04–0.15 Pa [Smith, 2002]. Sample vials were removed from the vacuum desiccator at scheduled time intervals, sealed immediately; weighed, and then analyzed using the laser Raman spectrometer.

A4. Phase Identification

[114] We monitored the progress of the hydration/dehydration process using noninvasive laser Raman spectroscopy and gravimetric measurements on the same sample at regular time intervals through the entire hydration/dehydration process. Some final products were selected for powder XRD, mid-IR ATR, and NIR diffuse reflectance spectroscopy measurements.

A4.1. In Situ Phase Identification Using Raman Spectroscopy

[115] Throughout the duration of the hydration/dehydration process, noninvasive Raman measurements were made on the samples at regular time intervals (Tables 2, 3, 4, 5, and 6). The measurement was made by focusing the excitation laser beam through the glass wall of a sealed reaction vial and by collecting the Raman-scattered light from the sample through the glass wall. Normally, three-point Raman checks were done on each sample to survey the homogeneity in hydration state of a sample. Three Raman measurements take only a few minutes to make. We did not see any changes in hydration state of Mg-sulfates owing to the sample temperature changes (from 50°C or 5°C to $\sim 21^\circ\text{C}$) during the short measurement interval. A HoloLab5000–532nm Raman spectrometer (Kaiser Optical Systems, Inc.) was used to obtain Raman spectra [Wang *et al.*, 2006c].

A4.2. Gravimetric Measurements

[116] A gravimetric (mass loss or gain) measurement was coupled with the Raman measurement on each sample. In this way, phase identification by Raman spectroscopy for each intermediate product of hydration/dehydration process is coupled with an average number of water molecules per MgSO_4 , calculated on the basis of gravimetric measurements. A Mettler PM480 DeltaRange[®] balance was used to make these measurements. We did not make XRD and IR measurements for the products at intermediate stages be-

cause these measurements require removal of samples from reaction vials.

A4.3. Structural Confirmation by XRD

[117] We used the Raman spectra of eleven standard Mg sulfates, hydrated and anhydrous, crystalline and amorphous [Wang *et al.*, 2006c] to identify pure hydrates or mixtures of the hydrates of Mg-sulfate occurring during and at the end of the hydration/dehydration process. We also took XRD measurements of the end products when there was need to confirm the phase identification indicated by Raman spectra. A Rigaku Geigerflex X-ray diffractometer with a CuK α radiation source was used for these measurements. Instrument details and the method used to prevent hydration state changes during XRD measurements are described by Wang *et al.* [2006c].

A4.4. IR Measurement for Typical Samples to Compare With Mission Spectra

[118] IR spectra were taken from the end products of some samples in this study. The IR spectrometer used for these measurements is an FT-IR spectrometer (Nexus 670 by Thermo Nicolet). The system has an infrared spectral region from 11000 cm^{-1} to 400 cm^{-1} (0.9 μm to 25 μm), which covers both the near IR spectral range of 0.9–5 μm used by OMEGA (Mars Express) and CRISM (Mars Reconnaissance Orbiter) for observing overtone and combination modes, and the mid-IR spectral range of 2.5–25 μm used by TES (Mars Global Surveyor), THEMIS (Mars Odyssey), and MiniTES (Mars Exploration Rovers) for observing the fundamental vibrational modes. The spectral resolution was set at 4 cm^{-1} , suitable for simulation studies. NIR diffuse reflectance measurements (0.9 μm to 25 μm) were made using a Harric Cricket reflectance attachment. The mid-IR ATR measurements were made using a diamond anvil ATR attachment.

[119] **Acknowledgments.** This work was supported by NASA funding NNX07AQ34G, Mars Fundamental Reach Program. We thank R. V. Morris for providing Fe-oxide and Fe-hydroxide samples. We thank I-Ming Chou for providing the phase boundary data and for instructive discussions. We thank R. E. Arvidson and K. A. Lichtenberg for providing typical OMEGA and CRISM spectra of polyhydrated sulfates and sulfate monohydrate. We also appreciate very much the instructive comments from two reviewers, I-Ming Chou and Nicolas Tosca, which helped us improve the manuscript.

References

- Arvidson, R. E. (2006), The sedimentary rocks exposed in Terra Meridiani, *Workshop on Martian Sulfates as Recorders of Atmospheric-Fluid-Rock Interactions*, LPI Contrib. 1331, Abstract 7043.
- Arvidson, R. E., *et al.* (2005), Spectral reflectance and morphologic correlations in eastern Terra Meridiani, Mars, *Science*, 307, 591–1593, doi:10.1126/science.1109509.
- Arvidson, R. E., *et al.* (2006a), Nature and origin of the hematite-bearing plains of Terra Meridiani based on analyses of orbital and Mars Exploration rover data sets, *J. Geophys. Res.*, 111, E12S08, doi:10.1029/2006JE002728.
- Arvidson, R. E., *et al.* (2006b), Overview of the Spirit Mars Exploration Rover mission to Gusev Crater: Landing site to the Backstay Rock in the Columbia Hills, *J. Geophys. Res.*, 111, E02S01, doi:10.1029/2005JE002499.
- Arvidson, R. E., *et al.* (2008), Introduction to special section on results from the Mars Exploration Rover Spirit and Opportunity missions, *J. Geophys. Res.*, 113, E06S01, doi:10.1029/2008JE003188.
- Bibring, J.-P., *et al.* (2006a), Mars surface diversity as observed by the OMEGA/Mars Express investigation, *Science*, 307, 1576–1581, doi:10.1126/science.1108806.
- Bibring, J.-P., *et al.* (2006b), Mars history derived from the mineralogical data of OMEGA/MEX acquired during the first Martian year of operation, *Lunar Planet. Sci.*, XXXVII, Abstract 2276.
- Bibring, J.-P., *et al.* (2006b), Global mineralogical and aqueous Mars history derived from OMEGA/Mars Express data, *Science*, 312, 400–404, doi:10.1126/science.1122659.
- Bish, D. L., J. W. Carey, D. T. Vaniman, and S. J. Chipera (2003), Stability of hydrous minerals on the Martian surface, *Icarus*, 164, 96–103, doi:10.1016/S0019-1035(03)00140-4.
- Bishop, J. L., *et al.* (2008), Phyllosilicate diversity and past aqueous activity revealed at Mawrth Vallis, Mars, *Science*, 321, 830–833, doi:10.1126/science.1159699.
- Blount, C. W., and F. W. Dickson (1973), Gypsum-anhydrite equilibria in systems CaSO₄-H₂O and CaSO₄-NaCl-H₂O, *Am. Mineral.*, 58, 323–331.
- Chipera, S. J., and D. T. Vaniman (2007), Experimental stability of magnesium sulfate hydrates that may be present on Mars, *Geochim. Cosmochim. Acta*, 71, 241–250, doi:10.1016/j.gca.2006.07.044.
- Chipera, S. J., J. W. Carey, and D. L. Bish (1997), Controlled humidity XRD analyses: Application to the study of smectite expansion/contraction, in *Advances in X-ray Analysis*, vol. 39, edited by J. V. Gilfrich *et al.*, pp. 713–722, Plenum, New York.
- Chou, I.-M., and R. R. Seal II (2003), Determination of epsomite-hexahydrate equilibria by the humidity-buffer technique at 0.1 MPa with implications for phase equilibria in the system MgSO₄-H₂O, *Astrobiology*, 3, 619–629, doi:10.1089/153110703322610708.
- Chou, I.-M., and R. R. Seal II (2007), Magnesium and calcium sulfate stabilities and the water budget of Mars, *J. Geophys. Res.*, 112, E11004, doi:10.1029/2007JE002898.
- Chou, I.-M., R. R. Seal II, and B. S. Hemingway (2002), Determination of melanterite-rozenite and chalcantite-bonattite equilibria by humidity measurements at 0.1 MPa, *Am. Mineral.*, 87, 108–114.
- Clark, B. C. (1993), Geochemical components in Martian soil, *Geochim. Cosmochim. Acta*, 57, 4575–4581, doi:10.1016/0016-7037(93)90183-W.
- Clark, B. C., *et al.* (1976), Inorganic analyses of Martian surface samples at the Viking landing sites, *Science*, 194, 1283–1288, doi:10.1126/science.194.4271.1283.
- Clark, B. C., *et al.* (1982), Chemical composition of Martian fines, *J. Geophys. Res.*, 87, 10,059–10,067, doi:10.1029/JB087iB12p10059.
- Clark, B. C., *et al.* (2005), Chemistry and mineralogy of outcrops at Meridiani Planum, *Earth Planet. Sci. Lett.*, 240, 73–94, doi:10.1016/j.epsl.2005.09.040.
- Deer, W. A., R. A. Howie, and J. Zussman (1966), *An Introduction to the Rock-Forming Minerals*, John Wiley, New York.
- Ehlmann, B. L., *et al.* (2008), Clay minerals in delta deposits and organic preservation potential on Mars, *Nat. Geosci.*, 1, doi:10.1038/ngeo207.
- Feldman, W. C., *et al.* (2004), The global distribution of near-surface hydrogen on Mars, *J. Geophys. Res.*, 109, E09006, doi:10.1029/2003JE002160.
- Freeman, J. J., A. Wang, and B. L. Jolliff (2007), Pathways to form kieserite from epsomite at mid-low temperatures, *Lunar Planet. Sci.*, XXXVIII, Abstract 1298.
- Freeman, J. J., M. Jin, and A. Wang (2008), D₂O substitution experiment on hydrated iron and magnesium sulfates and its application for spectral interpretation of Martian sulfates, *Lunar Planet. Sci.*, XXXIX, Abstract 2390.
- Gendrin, A., *et al.* (2005), Sulfates in Martian layered terrains: The OMEGA/Mars Express view, *Science*, 307, 1587–1591, doi:10.1126/science.1109087.
- Gooding, J. L., and K. Keil (1978), Alteration of glass as a possible source of clay minerals on Mars, *Geophys. Res. Lett.*, 5, 727–730, doi:10.1029/GL005i008p00727.
- Greenspan, L. (1977), Humidity fixed points of binary saturated aqueous solution, *J. Res. Natl. Bur. Stand. U.S., Sect. A*, 81A, 89–96.
- Hardie, L. A. (1967), The gypsum-anhydrite equilibrium at one atmosphere pressure, *Am. Mineral.*, 52, 171–200.
- Haskin, L. A., *et al.* (2005), Water alteration of rocks and soils from the Spirit rover site, Gusev Crater, Mars, *Nature*, 436, 66–69, doi:10.1038/nature03640.
- Hawthorne, F. C., *et al.* (1987), Kieserite, Mg(SO₄)(H₂O), a titanite-group mineral, locality: Wathlingen, Hanover, Germany, *Neues Jahrb. Mineral Abh.*, 157, 121–132.
- Hurowitz, J. A., *et al.* (2006), In situ and experimental evidence for acidic weathering of rocks and soils on Mars, *J. Geophys. Res.*, 111, E02S19, doi:10.1029/2005JE002515.
- Jambor, J. L., D. K. Nordstrom, and C. N. Alpres (2000), Metal-sulfate salts from sulfide mineral oxidation, in *Reviews in Mineralogy and Geochemistry*, vol. 40, *Sulfate Minerals: Crystallography, Geochemistry, and Environmental Significance*, edited by C. N. Alpres *et al.*, pp. 305–350, Mineral. Soc. of Am., Washington D. C.
- Langevin, Y., *et al.* (2005), Sulfates in the north polar region of Mars detected by OMEGA/Mars Express, *Science*, 307, 1584–1586, doi:10.1126/science.1109091.

- Lichtenberg, K. A., et al. (2008), Structural and geologic relationships between igneous rocks and their alteration products in Xanthe Terra, Mars, *Lunar Planet. Sci.*, XXXIX, Abstract 1390.
- Ling, Z. C., et al. (2008a), A systematic Raman, mid-IR, and vis-NIR spectroscopic study of ferric sulfates and implications for sulfates on Mars, *Lunar Planet. Sci.*, XXXIX, Abstract 1463.
- Ling, Z. C., et al. (2008b), A new phase of hydrated ferric sulfates, lausenite?, paper presented at 8th International Conference on Raman Spectroscopy Applied to Earth Science, Russian Mineral. Soc., Ghent, Belgium.
- Mangold, N., et al. (2006), Sulfate deposits and geology of West Candor Chasma, a case study, *Workshop on Martian Sulfates as Recorders of Atmospheric-Fluid-Rock Interactions*, LPI Contrib. 1331, Abstract 7043.
- Mangold, N., et al. (2007), An overview of the sulfates detected in the equatorial regions by the OMEGA/MEX spectrometer, paper presented at 7th International Conference on Mars, Abstract 3141, Lunar Planet. Sci., Pasadena, Calif.
- McLennan, S. M., et al. (2007), Geochemistry, mineralogy and diagenesis of the Burns Formation at Meridiani Planum: Insights into the sedimentary rock cycle on Mars, in *Seventh International Conference on Mars*, July 9–13, 2007, Pasadena CA, LPI Contrib. 1358, Abstract 3231.
- McSween, H. Y., et al. (2004), Basaltic rocks analyzed by the Spirit rover in Gusev Crater, *Science*, 305, 842–845, doi:10.1126/science.3050842.
- McSween, H. Y., et al. (2006), Characterization and petrologic interpretation of olivine-rich basalts at Gusev Crater, Mars, *J. Geophys. Res.*, 111, E02S10, doi:10.1029/2005JE002477.
- Mellon, M. T., W. C. Feldman, and T. H. Prettyman (2004), The presence and stability of ground ice in the southern hemisphere of Mars, *Icarus*, 169, 324–340, doi:10.1016/j.icarus.2003.10.022.
- Ming, D. W., et al. (2006), Geochemical and mineralogical indicators for aqueous processes in the Columbia Hills of Gusev Crater, Mars, *J. Geophys. Res.*, 111, E02S12, doi:10.1029/2005JE002560.
- Ming, D. W., et al. (2008), Geochemical properties of rocks and soils in Gusev Crater, Mars: Results of the Alpha Particle X-Ray Spectrometer from Cumberland Ridge to Home Plate, *J. Geophys. Res.*, 113, E12S39, doi:10.1029/2008JE003195.
- Møller, N. (1988), The prediction of mineral solubilities in natural waters: A chemical equilibrium model for the Na-Ca-Cl-SO₄-H₂O system, to high temperature and concentration, *Geochim. Cosmochim. Acta*, 52, 821–837, doi:10.1016/0016-7037(88)90354-7.
- Morris, R. V., et al. (2006a), Mössbauer mineralogy of rock, soil, and dust at Gusev Crater, Mars: Spirit's journey through weakly altered olivine basalt on the plains and pervasively altered basalt in the Columbia Hills, *J. Geophys. Res.*, 111, E02S13, doi:10.1029/2005JE002584.
- Morris, R. V., et al. (2006b), Mössbauer mineralogy of rock, soil, and dust at Meridiani Planum, Mars: Opportunity's journey across sulfate-rich outcrop, basaltic sand and dust, and hematite lag deposits, *J. Geophys. Res.*, 111, E12S15, doi:10.1029/2006JE002791.
- Morris, R. V., et al. (2008), Iron mineralogy and aqueous alteration from Husband Hill through Home Plate at Gusev Crater, Mars: Results from the Mössbauer instrument on the Spirit Mars Exploration Rover, *J. Geophys. Res.*, 113, E12S42, doi:10.1029/2008JE003201.
- Murchie, S., et al. (2007a), CRISM mapping of layered deposits in western Candor Chasma, paper presented at 7th International Conference on Mars, Abstract 3238, Lunar Planet. Sci., Pasadena, Calif.
- Murchie, S., et al. (2007b), Compact reconnaissance imaging spectrometer for Mars (CRISM) on Mars reconnaissance orbiter (MRO), *J. Geophys. Res.*, 112, E05S03, doi:10.1029/2006JE002682.
- Mustard, J. F., et al. (2008), Hydrated silicate minerals on Mars observed by the Mars reconnaissance orbiter CRISM instrument, *Nature*, 454, 305–309, doi:10.1038/nature07097.
- Nesbitt, H. W., and R. E. Wilson (1992), Recent chemical weathering of basalts, *Am. J. Sci.*, 292, 740–777.
- Nesbitt, H. W., and G. M. Young (1984), Prediction of some weathering trends of plutonic and volcanic rocks based on thermodynamic and kinetic considerations, *Geochim. Cosmochim. Acta*, 48, 1523–1534, doi:10.1016/0016-7037(84)90408-3.
- Papike, J. J., et al. (2008), Mars surface mineralogy: Kieserite MgSO₄·H₂O: Characterization of a terrestrial end-member, *Lunar Planet. Sci.*, XXXIX, Abstract 1001.
- Peterson, R. C., and R. Wang (2006), Crystal molds on Mars: Melting of a possible new mineral species to create Martian chaotic terrain, *Geology*, 34, 957–960, doi:10.1130/G22678A.1.
- Roach, L., et al. (2007), Magnesium and iron sulfate variety and distribution in east Candor and Capri Chasma, Valles Marineris, paper presented at 7th International Conference on Mars, Abstract 3223, Lunar Planet. Sci., Pasadena, Calif.
- Roach, L., et al. (2008), Constraints on the rate of sulfate phase changes in Valles Marineris interior layered deposits, *Lunar Planet. Sci.*, XXXIX, Abstract 1823.
- Ruff, S. W. (2004), Spectral evidence for zeolite in the dust on Mars, *Icarus*, 168, 131–143, doi:10.1016/j.icarus.2003.11.003.
- Ruff, S. W., et al. (2006), The rocks of Gusev Crater as viewed by the Mini-TES instrument, *J. Geophys. Res.*, 111, E12S18, doi:10.1029/2006JE002747.
- Smith, M. D. (2002), The annual cycle of water vapor on Mars as observed by the thermal emission spectrometer, *J. Geophys. Res.*, 107(E11), 5115, doi:10.1029/2001JE001522.
- Smith, M. D., et al. (2004), First atmospheric science results from the Mars Exploration Rovers Mini-TES, *Science*, 306, 1750–1753.
- Smith, M. D., et al. (2006), One Martian year of atmospheric observations using MER Mini-TES, *J. Geophys. Res.*, 111, E12S13, doi:10.1029/2006JE002770.
- Squyres, S. W., et al. (2006a), Overview of the Opportunity Mars Exploration Rover mission to Meridiani Planum: Eagle crater to purgatory ripple, *J. Geophys. Res.*, 111, E12S12, doi:10.1029/2006JE002771.
- Squyres, S. W., et al. (2006b), Rocks of the Columbia Hills, *J. Geophys. Res.*, 111, E02S11, doi:10.1029/2005JE002562.
- Squyres, S. W., et al. (2007), Pyroclastic activity at Home Plate in Gusev Crater, Mars, *Science*, 316, 738–742.
- Tosca, N. J., and S. M. McLennan (2006), Chemical divides and evaporite assemblages on Mars, *Earth Planet. Sci. Lett.*, 241, 21–31, doi:10.1016/j.epsl.2005.10.021.
- Tosca, N. J., et al. (2004), Acid-sulfate weathering of synthetic Martian basalt: The acid fog model revisited, *J. Geophys. Res.*, 109, E05003, doi:10.1029/2003JE002218.
- Tosca, N. J., S. M. McLennan, B. C. Clark, J. P. Grotzinger, J. A. Hurowitz, A. H. Knoll, C. Schröder, and S. W. Squyres (2005), Geochemical modeling of evaporation processes on Mars: Insight from the sedimentary record at Meridiani Planum, *Earth Planet. Sci. Lett.*, 240, 122–148, doi:10.1016/j.epsl.2005.09.042.
- Tosca, N. J., et al. (2008), Fe oxidation processes at Meridiani Planum and implications for secondary Fe mineralogy on Mars, *J. Geophys. Res.*, 113, E05005, doi:10.1029/2007JE003019.
- Vaniman, D. T., and S. J. Chipera (2006), Transformation of Mg- and Ca-sulfate hydrates in Mars regolith, *Am. Mineral.*, 91, 1628–1642, doi:10.2138/am.2006.2092.
- Vaniman, D. T., et al. (2004), Magnesium sulphate salts and the history of water on Mars, *Nature*, 431, 663–665, doi:10.1038/nature02973.
- Vaniman, D. T., S. J. Chipera, and J. W. Carey (2006), Hydration experiments and physical observations at 193 K and 243 K for Mg-sulfates relevant to Mars, *Lunar Planet. Sci.*, XXXVII, Abstract 1442.
- Wang, A., et al. (2006a), Evidence of phyllosilicates in woolly patch, an altered rock encountered at west spur, Columbia Hills, by the Spirit Rover, *J. Geophys. Res.*, 111, E02S16, doi:10.1029/2005JE002516.
- Wang, A., et al. (2006b), Sulfate deposition in subsurface regolith in Gusev Crater, Mars, *J. Geophys. Res.*, 111, E02S17, doi:10.1029/2005JE002513.
- Wang, A., et al. (2006c), Sulfates on Mars: A systematic Raman spectroscopic study of hydration states of magnesium sulfates, *Geochim. Cosmochim. Acta*, 70, 6118–6135.
- Wang, A., J. J. Freeman, and B. L. Jolliff (2007), Formation rate of amorphous magnesium sulfates at low temperatures approaching the current surface conditions on Mars, *Lunar Planet. Sci.*, XXXVIII, Abstract 1195.
- Wang, A., et al. (2008a), Light-toned salty soils and coexisting Si-rich species discovered by the Mars Exploration Rover Spirit in Columbia Hills, *J. Geophys. Res.*, 113, E12S40, doi:10.1029/2008JE003126.
- Wang, A., J. J. Freeman, and R. E. Arvidson (2008b), Study of two structural polymorphs of MgSO₄·H₂O by Raman, IR, XRD, and humidity buffer experiments: Implication for Martian kieserite, *Lunar Planet. Sci.*, XXXIX, Abstract 2172.
- White, W. B. (1974), Order-disorder effects, in *The Infrared Spectra of Minerals*, Mineral. Soc. Monogr., vol. 4, edited by V. C. Farmer, pp. 87–110, Mineral. Soc., London.
- Wiseman, S. M., et al. (2007), New analyses of MRO CRISM, HIRISE, and CTX data over layered sedimentary deposits in Meridiani, paper presented at 7th International Conference on Mars, Abstract 3111, Lunar Planet. Sci., Pasadena, Calif.
- Yen, A. S., et al. (2008), Hydrothermal processes at Gusev Crater: An evaluation of paso robles class soils, *J. Geophys. Res.*, 113, E06S10, doi:10.1029/2007JE002978.
- Zheng, M. P. (1997), *An Introduction to Saline Lakes on the Qinghai-Tibet Plateau*, Kluwer Acad., Dordrecht, Netherlands.

J. J. Freeman, B. L. Jolliff, and A. Wang, Department of Earth and Planetary Sciences and the McDonnell Center for the Space Sciences, Washington University, St. Louis, MO 63130, USA. (alianw@levee.wustl.edu)